ANALYSIS OF THE OVER-STATION BEHAVIOUR OF THE AIRBORNE ADF SYSTEM

HERBERT HAMILTON WARD III

for the degree of

MASTER OF SCIENCE

IN

ENGINEERING ELECTRONICS

United States Naval Postgraduate School

Monterey, California

1 9 5 4

This work is accepted as fulfilling

the thesis requirements for the degree of

MASTER OF SCIENCE

in

ENGINEERING ELECTRONICS

from the

United States Naval Postgraduate School

ABSTRACT

A theoretical investigation is made of the behavior of low-frequency radio compass systems in aircraft on courses near and over the radio station. This behavior is explained in the light of electromagnetic field theory and the equipment characteristics. An equation is derived for the locus of all points where the radio compass indicator will start to reverse due to sense antenna signal phase shift with respect to the loop antenna signal as the station axis is approached and passed. The equation contains six geometrical and electrical variables. The locus thus defined is similar to a cone or paraboloid, apex down, with the apex located at the radio station in most cases.

The equation predicts that for a phase advance of the loop signal, relative to the sense antenna signal, of slightly more than the 90 degree value applied by the basic ideal receiver, the apex of the cone-like space figure locus rises off the ground. It should then be possible to fly under this apex producing but one reversal of the ADF indicator needle with this single reversal starting exactly over the radio station. The altitude of this apex is a relatively simple function of the variables.

The results of the flight tests verifying the theoretical findings are given together with some requisites for the use of the findings to eliminate the effects due to improper sense antenna location provided the location error is not too extreme.

PREFACE

This investigation was undertaken by the writer while a student at the United States Naval Postgraduate School located at Monterey, California, and while on duty at the Stanford Research Institute in Stanford, California, during a ten week industrial experience tour. This industrial experience program is a regular part of the Electronics Engineering Curriculum of the Naval Postgraduate School. It is made possible by the continued cooperation of the members of the Electronics Industry who take these naval-officer students into their organizations to familiarize them with the workings of the industry.

The writer is very much indebted to the staff of the Radio Systems Laboratory of Stanford Research Institute for the cheerful cooperation and many services rendered this student in their midst. Especially is he indebted to Dr. J. T. Bolljahn for the friendly council given during our many conversations and to Mr. Vincent Kelly for his assistance during the flight test phases of the project. The atmosphere of research created in the Radio Systems Laboratory is an inspiration to all who work there.

Finally, I wish to express my deep gratitude to my wife, Kathryn, without whose patient indulgence and encouragement my three years of belated scholastic endeavor would not have been possible.

Herbert H. Ward 3rd

Menlo Park, California

March 1954

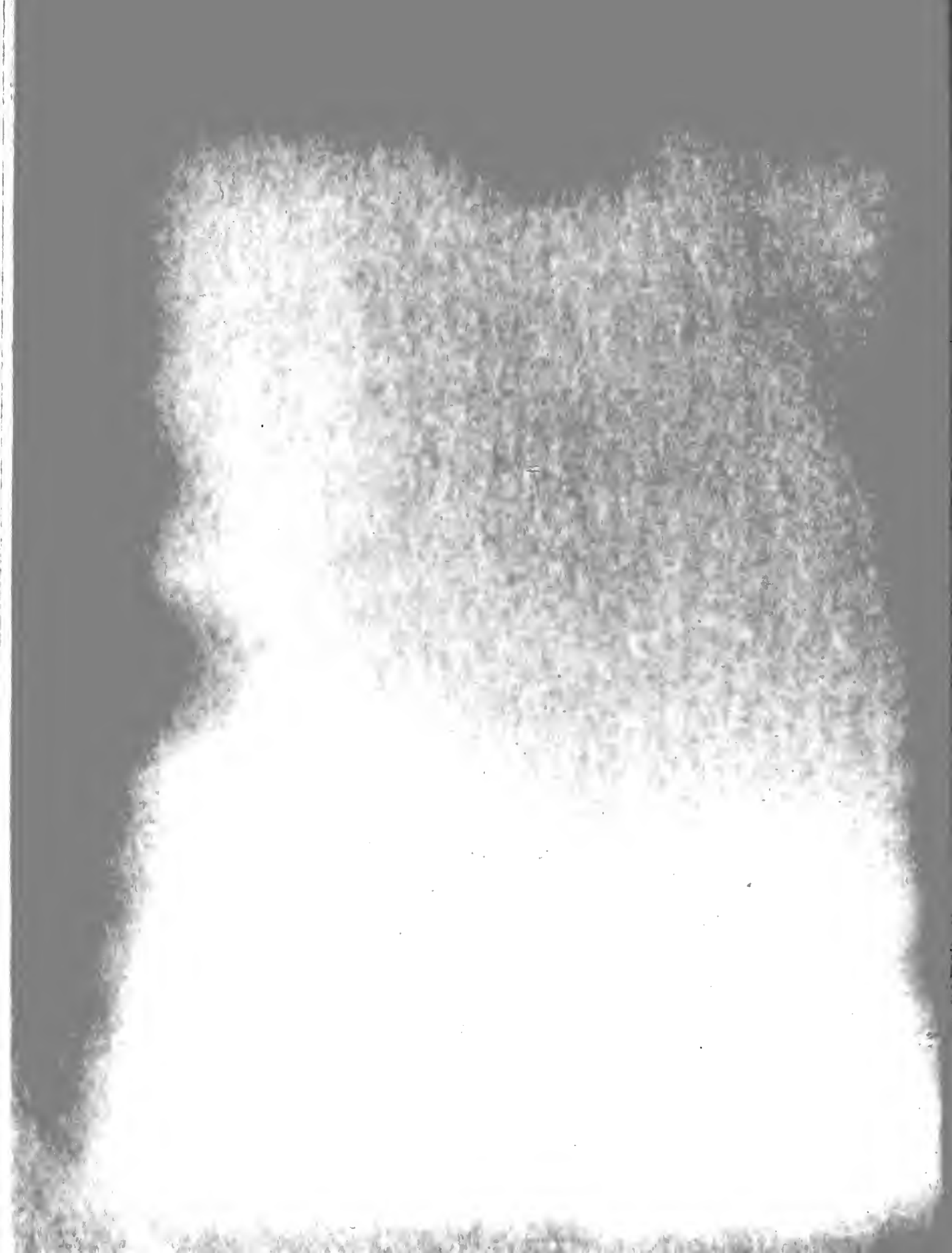

TABLE OF CONTENTS

LIST OF FIGURES

TABLE OF SYMBOLS

A	$\pi \tan \gamma$; also used to designate planes or flight paths on figures
B	used to designate planes or flight paths on figures
b	the minimum horizontal distance, expressed in wavelengths, between the vertical axis of the radio station and the aircraft flight path, $b = d/\lambda$ (see Fig. 3)
C	capacitance
c	velocity of propagation of electromagnetic waves
D	$\sin \theta (\cos \theta \tan \alpha - \sin \theta)$
d	the minimum horizontal distance between the vertical axis of the radio station and the aircraft flight path (see Fig. 3)
E	electric field intensity
e	a point on various figures
f	frequency
H	magnetic field intensity
h	altitude expressed in wavelengths, $h = z/\lambda$
I	current
j	$\sqrt{-1}$
K	$h \tan \alpha$
k	a constant
l	length
n	any number
p	the horizontal distance, expressed in wavelengths, from the station axis to the airplane, $p = \rho/\lambda$
R	resistance
r	the distance from the station to the aircraft
ρ	the distance, in wavelengths, from the station to the aircraft, $\rho = r/\lambda$
S	area

t	time
U	$\left(1 - j\frac{\lambda}{2\pi r}\right)\epsilon^{j(\omega t - \beta r)}$
V_l	loop antenna voltage
V_l	loop antenna voltage after it has been advanced γ° by the receiver
V_s	sense antenna voltage per unit length
x	horizontal dimension in rectangular coordinate system, (see Fig. 3)
y	altitude
α	tilt angle of effective sense antenna
β	phase constant
γ	phase shift applied to loop antenna signal by receiver
Δ	error in the phase of V_s caused by not considering the third term of E_θ.
δ	$\frac{\lambda}{2\pi r}$ $\left(= \frac{1}{2\pi\lambda}\right)$
ϵ	base of natural logarithms
η	intrinsic impedance of propagating medium
θ	vertical angle in coordinate system (see Fig. 3)
λ	wavelength
μ	magnetic permeability
π	3.1415·····
ρ	the horizontal distance from the station axis to the airplane
σ	a phase shift angle
ϕ	horizontal angle in coordinate system (see Fig. 30)
ω	$2\ \pi\ f$
$\angle$	"the phase angle of"

CHAPTER I

INTRODUCTION

1. The Radio Compass and the Problem.

The family of Airborne Radio Compasses Manufactured by the Bendix Radio Division of the Bendix Aviation Corporation and others have been guiding aircraft safely toward and over ground (and shipborne) Low Frequency radio stations for many years. The Bendix NA-1, AN/ARN-7, AN/ARN-6, SCR-269, and BC-433 are a few notable members of this family. All the family are referred to as the "A.D.F.", for Automatic Direction Finder, throughout most of the Aviation world and are more familiarly called the "Bird-dog" by many.

One primary function of the ADF is to point in the direction of any selected radio station transmitting in the frequency range of from 100 to 1750 kilocycles per second (kc). The aircraft pilot or navigator may then direct his course toward the station or may determine his bearing from the station to be used as one line of position in determining his geographical position.

The characteristics of a radio wave that presumably could be determined by an aircraft in flight, properly instrumented, would be its frequency, amplitude (or signal strength), polarization, the direction from which it is coming, and, if it is a modulated signal, the modulation and the intelligence contained therein. The aircraft would have to be traveling at 360 knots to change the apparent frequency by one ops even at the high frequency end of the ADF band. As this shift of frequency would be hard to detect in any case, frequency would appear to be a poor characteristic to check for directional information.

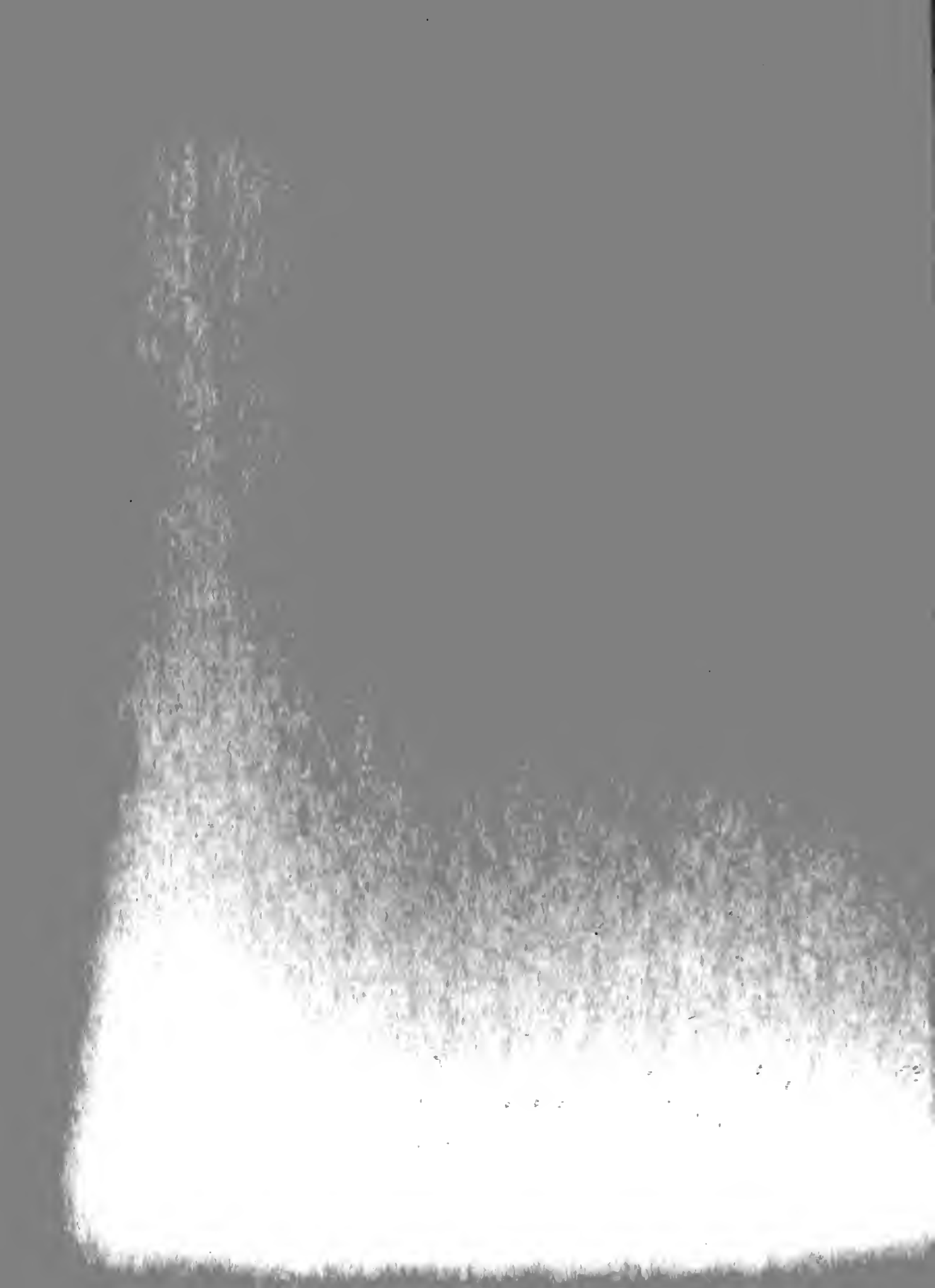

The signal strength will build or fade as the aircraft approaches or proceeds away from the radio station. This would give only a general indication of the station direction and would take a long time especially at appreciable ranges from the station even if used in conjunction with the sector identification if the station were a radio range. The polarization would give virtually no directional information. The modulation is used to give directional information in other homing systems where different codes are sent out on different bearings. The ADF, however, is designed to work with any station in the frequency range. It is not surprising, therefore, that the best directional information is given by determining the direction from which the signal is approaching the aircraft. This method suffers at long range from apparent shift of direction caused by reflection of the signal from mountains or other terrestrial features, and from atmospheric disturbances. However, at medium ranges the ADF systems in use do give relatively good performance. The current U.S. Air Force specification[8*] for the ADF calls for satisfactory performance under good conditions up to a minimum range of 130 miles from the station. Research is being carried out by the Stanford Research Institute and by others to improve the long range performance of the ADF.

There is another type of error to which the ADF is susceptible and this is the subject of our investigation. On courses near and over the radio station, the radio compass appears to be confused for a time, not knowing when it has passed the station. It will point first ahead then start to turn around, then it may return to the ahead bearing and finally turn around. Another time it may completely turn around the

* All superscripts in the text refer to numbered references in the bibliography.

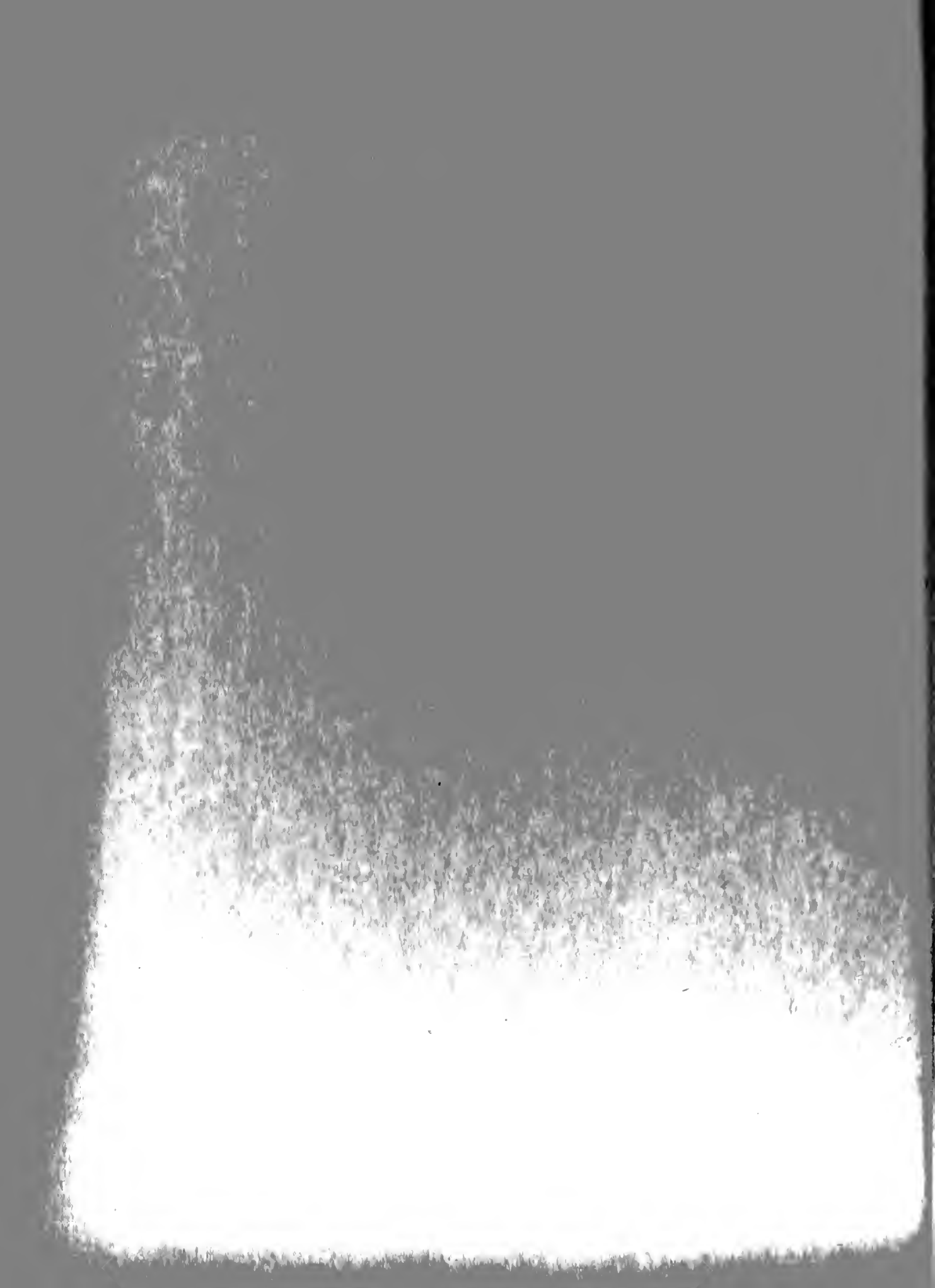

first time, return to the ahead bearing, and then finally point astern. There are other performances which have been observed. Lockhead, Douglas, and others have actually recorded the gyrations of the confused radio compass needle together with a record of the actual position of the aircraft relative to the station. This area of indecision has been given the name "The zone of confusion". Our purpose is to explain this zone of confusion in the light of electromagnetic field theory and the equipment characteristics. We will also describe what seems to be the most practical system of eliminating it entirely from the ground up to an altitude where the actual position inaccuracy caused by the zone of confusion is of little consequence. This system has been successfully tested in actual flight tests using simple equipment in addition to the ADF normally installed in the aircraft. The results of the tests and the equipment used are both described in this report.

2. Functioning of the ADF Receiver.

It is not our purpose here to give a complete and accurate description of the functioning of the various radio compasses but rather to point out the common characteristics which will have a bearing on our treatment of the problem. For more complete information reference is made to the respective instruction books.[9,10,11,12]

Referring to Fig. 1 we see depicted a loop of wire in a vertical plane so pivoted that its axis may be rotated in a horizontal plane. It is shown in a vertically polarized radiated field such as that from a vertical radiator and at some distance from the radiator. Here the magnetic field, H_ϕ, which is actually tangent to a horizontal circle with the station axis as a center, is essentially plane; and the electric field, E_θ, which is actually tangent to a vertical circle with

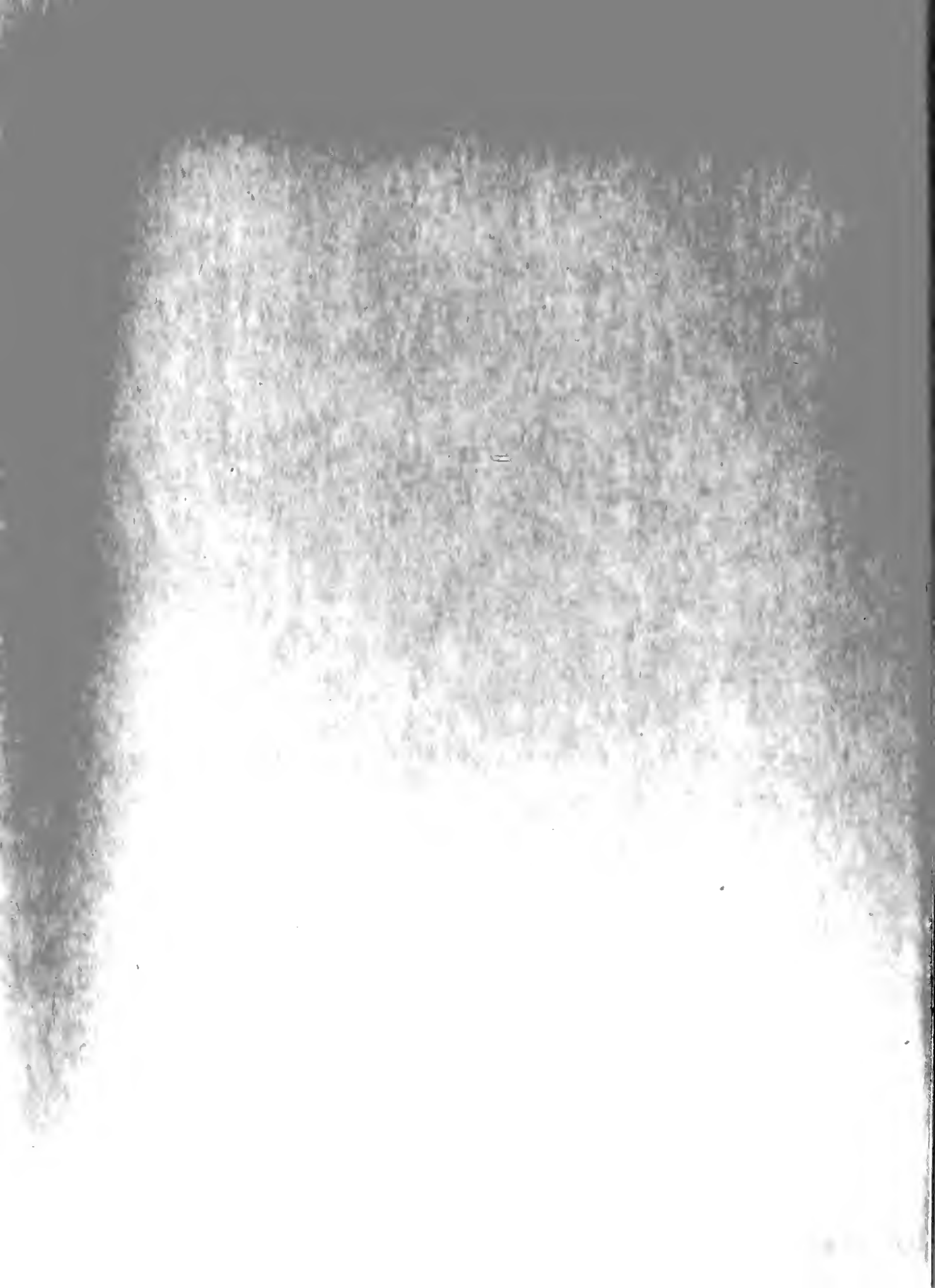

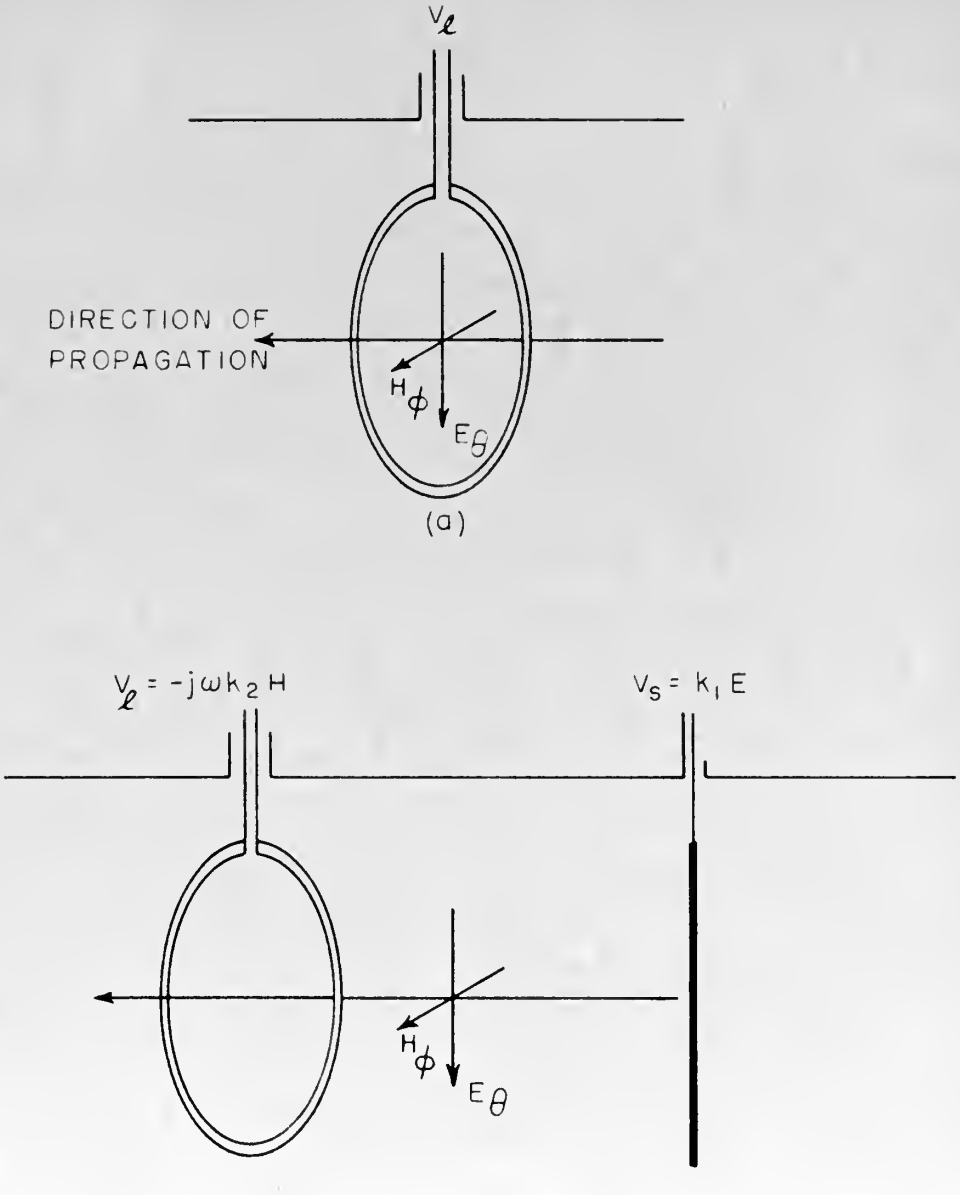

FIG. 1

BASIC LOOP AND SENSE ANTENNA OF
THE AUTOMATIC DIRECTION FINDER

A-591-TR40-408

the station as a center, is also essentially plane forming the elements of a plane wave. If the loop is turned so that its edge is toward the source of radiation, the maximum amount of magnetic flux will thread through the loop and the induced voltage will be a maximum. If the loop is turned so that it is in a plane perpindicular to the direction from which the radiation is coming, no magnetic flux will thread through the loop and the voltage induced in the loop will be zero. If we were to provide a servo amplifier and motor to drive the loop until the induced voltage was zero, we would have an automatic direction finder except that there are two positions, 180° apart, where the induced signal is zero. However, if we now make the servo amplifier phase sensitive, we will be able to make the servo amplifier determine from which direction the signal is coming. If the loop is oriented with its axis toward the station and is then rotated slightly clockwise, the signal will increase in magnitude. If the loop were rotated instead slightly counter-clockwise, the magnetic field would thread through the loop from the opposite side. The signal would increase as before but 180° out of phase with the first case. All that is needed is a phase reference voltage for the servo amplifier. To get this we need only put a simple whip or other antenna in the vicinity of the loop. The phase of the voltage induced in this "sense" antenna by the E_{θ} field is not affected by the motion of the loop. It is a characteristic of the radiation under consideration that the electric field and magnetic field are in time phase and, as indicated, in space quadrature. However, the voltage induced in the loop lags the H field by 90°. ($V_{\ell} = -jw\mu HS$[7], where S is the projected area through which H_{ϕ} passes.

This is the reason why V_l is a minimum when the face of the loop is toward the station.) The receiver advances the phase of the loop voltage by an angle γ, nominally 90°, and "compares" it with the sense antenna voltage. If it is then approximately in phase with the sense voltage, the receiver tells the servo motor to drive the loop one way to reduce the loop voltage to zero. If it is approximately in phase opposition to the sense voltage, the receiver tells the servo motor to drive the loop in the other direction to reach minimum loop voltage. We now have an automatic direction finder which has no 180° ambiguity and a simplified explanation of its theory of operation.

3. The Aircraft and the Sense Antenna.

Regardless of the type of antenna used on an aircraft as the ADF sense antenna, the investigations of Bolljahn[2,3], and Hoblitzell[6] have shown that, in the frequency range under consideration, the pattern of the aircraft-antenna combination will be that of a simple short dipole. The orientation of this dipole pattern depends on where the electrical center of the antenna is located relative to the electrical center of the airplane. If the antenna is located directly under or directly over the electrical center then the axis of the dipole pattern will be vertical. If the antenna is located below and forward or above and aft of the electrical center, the axis of the dipole will point forward and down. This we shall take as a positive sense antenna tilt angle. We shall call this angle " α " and meet it often. See Figure 2 for the variation of tilt angle with sense antenna location.

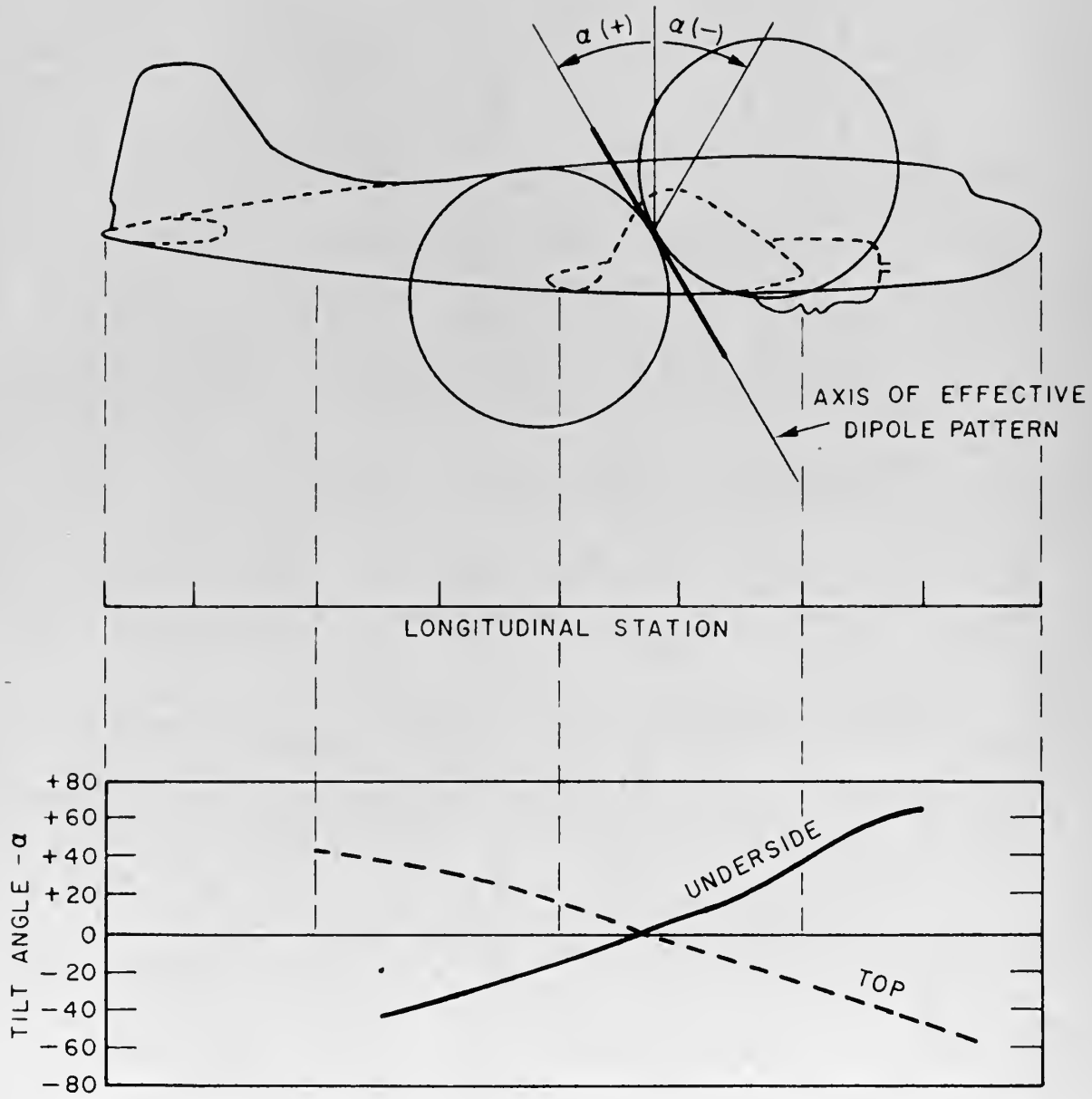

FIG. 2

TILT ANGLE OF SENSE ANTENNA VS LOCATION
ON DC-3 AIRCRAFT

A-591-TR40-409

This characteristic of the sense antenna poses several problems. With a positive tilt angle and a flight path directly over the station, we would expect from simple far field theory (considering only E_θ and H_ϕ) that the sense antenna would have two points of zero signal, one when the antenna pattern axis (null) crosses the transmitting station and one when the aircraft passes the null of the ground antenna; i.e. when the aircraft is directly over the station. At these two zero points the phase of the sense antenna voltage would reverse. The phase reversal which occurs directly over the station is compensated for by a simultaneous phase reversal in the loop signal and hence does not cause a reversal of the ADF indicator. The reversal due to the passage of the sense antenna null through the ground antenna location will cause a reversal of the indicator. Of course the problem is not as simple as this and the assumption of the far-field simplification is not valid. However we shall see that, if the tilt angle could be made zero, the performance would obviously be improved since the zone of confusion is reduced in size because any effect due to the sense antenna null occurs nearer the station passage.

We see from Fig. 2 that to have a near zero tilt angle we would have to locate the sense antenna back near the wing root on the centerline of the aircraft. This rule has proven to hold for all large aircraft types tested.[6] After locating the sense antenna here we would either have to locate the compass receiver in this location also or provide a cable inside the ship leading to the forward location of the actual compass receiver. The former solution is objected to by the commercial aircraft industry on the grounds that they want all of the radio gear in one place for ease of servicing and for standardization. The latter solution has

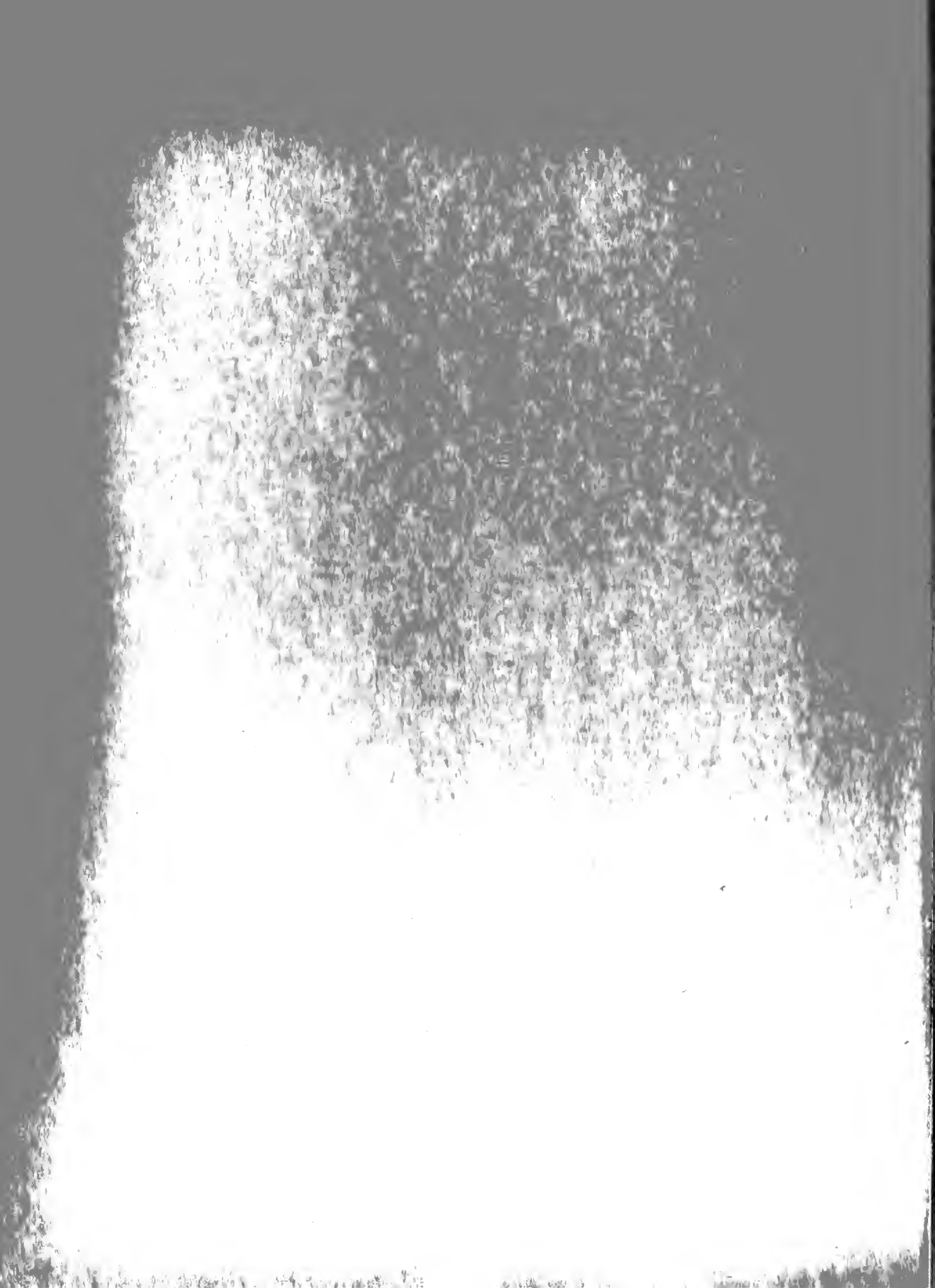

the disadvantage that the losses in a long cable, some 70 feet in the case of the larger aircraft, either reduces the sensitivity of the ADF at long ranges and therefore its performance or requires the use of a larger antenna with the structural problems attendant thereupon.

The modern trend to make all the antennas flush mounted or cavity types to reduce the drag in high speed aircraft,[5] coupled with the necessity of having the sense cavity either under the wing or on top of the aircraft over the wing to produce a small tilt angle, places the cavity in one of the most congested and structurally important areas of the aircraft.

Various solutions to this problem are being sought by the aircraft industry and through its research affiliations. One which is receiving some attention at present is the use of a unity gain matching device at the antenna end of the cable to minimize the effect of cable capacitance.[1] Another answer might be to provide two sense antennas. One small one under the wing, to be used close-in where the signal strength is high and therefore where cable loss would present no problem, and another of maximum efficiency adjacent to the radio rack to be used when extreme range maximum performance is needed. The shift from one to the other could be made by signal strength variation, the reaction time of the switching device being long enough that tuning operations and cone of silence passages would not activate it.

To summarize the above paragraphs, if the performance of the radio compass could be made independent of the tilt angle of the sense antenna pattern for reasonably small tilt angles then the problem of the placement of the sense antenna could be vastly simplified.

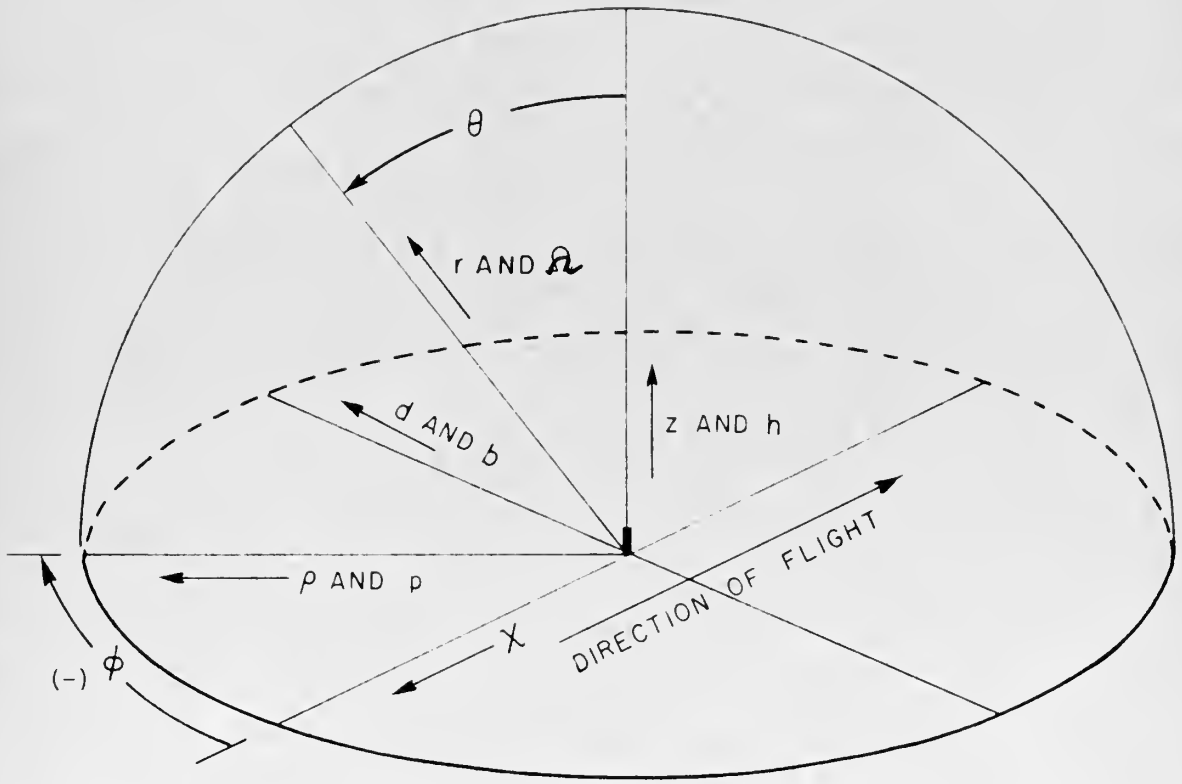

NOTE: ρ, d, r, z IN FEET
p, b, $\mathfrak{R}$, h IN WAVELENGTHS

FIG. 3

SYSTEMS OF COORDINATES USED

(RADIO STATION AT ORIGIN)

A-591-TR40-410

CHAPTER II

DERIVATION

1. Field Considerations.

Before proceeding with our analysis, it would be well to refer to Fig. 3 to take note of the systems of coordinates and the positive directions of the variables to be used throughout this work. The aircraft will always be assumed to be flying from left to right, from the positive x direction toward the negative x direction. The radio station will always be at the origin of the coordinate systems and will be shown as a small vertical element in many figures, as in Fig. 3.

As is shown in Fig. 4 (a) we have an aircraft flying in the radiated field of an electrically short vertical radiator. For all practical purposes we can say that this is the field of a current element for the antenna is generally short relative to a quarter wavelength and the effective current is of essentially one phase. Taking the field equations from Schelkunoff and Friis[7] and re-arranging slightly we have:

$$E_\theta = \frac{j\eta I_s}{2\lambda r}\left(1 - j\frac{\lambda}{2\pi r} - \frac{\lambda^2}{4\pi^2 r^2}\right) \epsilon^{j(\omega t - \beta r)} \sin\theta \qquad (1)$$

$$H_\phi = \frac{j I_s}{2\lambda r}\left(1 - j\frac{\lambda}{2\pi r}\right) \epsilon^{j(\omega t - \beta r)} \sin\theta \qquad (2)$$

$$E_r = \frac{\eta I_s}{2\pi r^2}\left(1 - j\frac{\lambda}{2\pi r}\right) \epsilon^{j(\omega t - \beta r)} \cos\theta \qquad (3)$$

Disregarding the third term of E_θ (see the APPENDIX)

$$E_\theta = \frac{j\eta I_s}{2\lambda r} U \sin\theta \qquad (4)$$

$$H_\phi = \frac{j I_s}{2\lambda r} U \sin\theta \qquad (5)$$

$$E_r = \frac{\eta I_s}{2\pi r^2} U \cos\theta \qquad (6)$$

where $$U = \left(1 - j\frac{\lambda}{2\pi r}\right) \epsilon^{j(\omega t - \beta r)} \qquad (7)$$

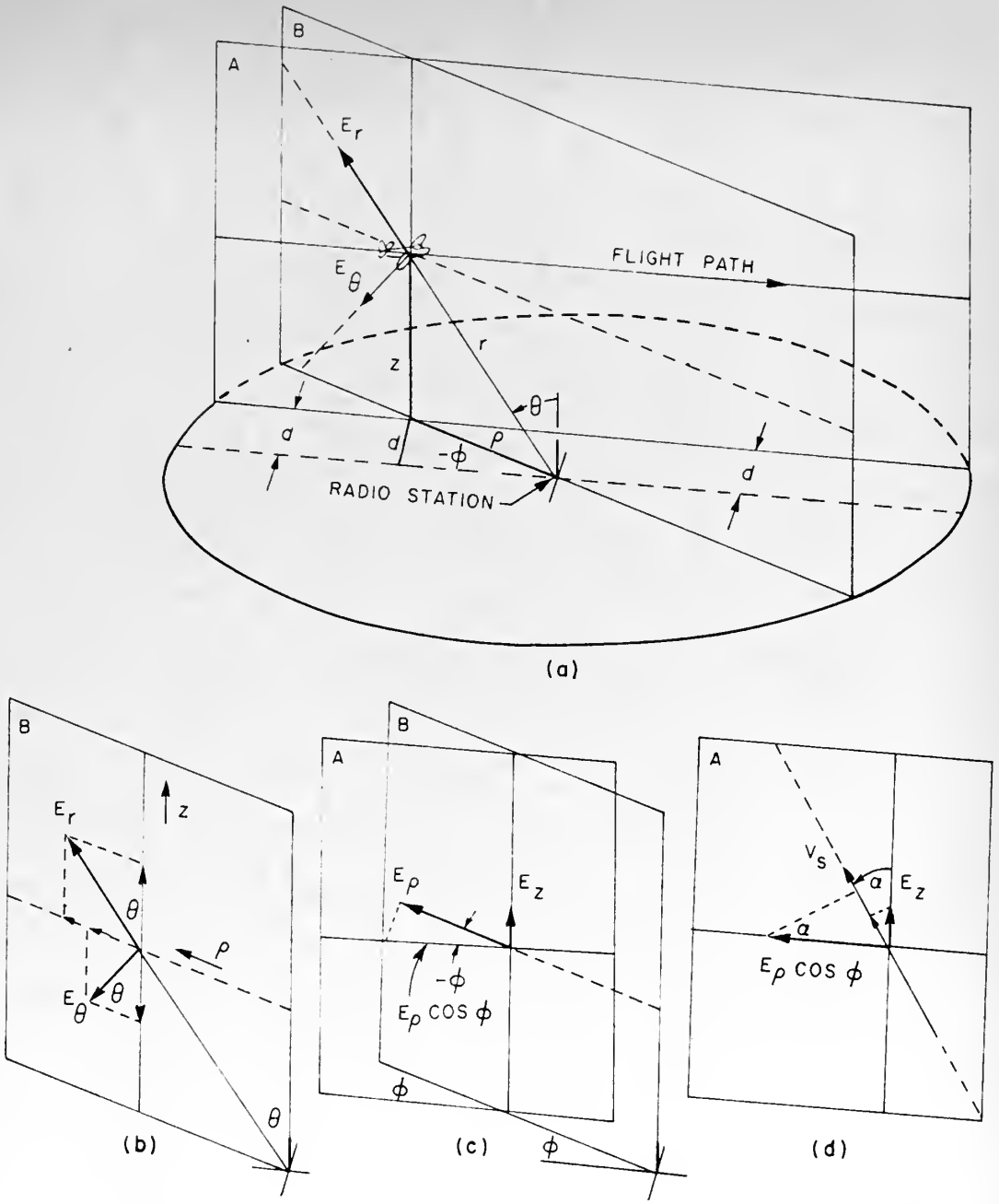

$E_\rho = E_r \sin\theta + E_\theta \cos\theta$

$E_z = E_r \cos\theta - E_\theta \sin\theta$

$V_s = E_z \cos\alpha + (E_\rho \cos\phi) \sin\alpha$

V_s IS THE VOLTAGE IN THE SENSE ANTENNA, PER UNIT LENGTH

α IS THE TILT ANGLE OF THE EFFECTIVE SENSE ANTENNA

FIG. 4

PLANES SHOWING FIELD VECTORS

8-591-TR40-411

The time phase relations of these field quantities are shown in Fig.5.

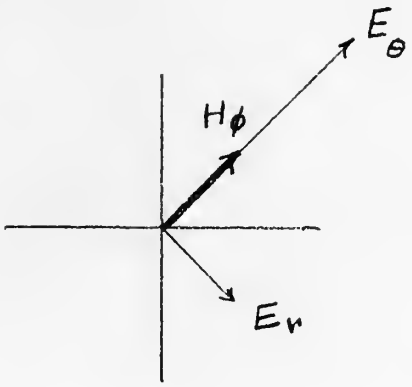

Fig. 5
Phase Relations of
Basic Field Quantities.

The phase angle between the voltages induced in the loop and sense antenna depends, of course, upon the location of the receiving system (r, θ) and upon the orientation of the sense antenna, which fixes the relative amounts of E_θ and E_r which act upon the antenna.

At great distances horizontally from the antenna, in the area called the "far field or radiated field"[7] of the current element, $E_r \ll E_\theta$ in as much as $E_r \propto \frac{1}{r^2}$ while $E_\theta \propto \frac{1}{r}$ and also due to the fact that $\theta \approx 90^\circ$. Even near the station for points near the ground, $\theta \approx 90^\circ$ and hence $E_r \ll E_\theta$. However our investigation is specifically concerned with the area where θ may have any value from 0° to 90° and in the "near field"[7] of the radiating element. Under these conditions $|E_r|$ may be equal to or greater than $|E_\theta|$.

As suggested by Schelkunoff and Friis:[7] let $r \sin\theta = \rho$ then

$$E_\theta = \frac{j \eta I_s U}{2 r^2} \cdot \frac{\rho}{\lambda} \qquad (4a)$$

$$E_r = \frac{\eta I_s U}{2 r^2} \cdot \frac{\cos\theta}{\pi} \qquad (6a)$$

where ρ is the horizontal distance from the vertical radiator axis to the point under consideration. If $\rho \leq \frac{\lambda}{\pi} \cos\theta$ then $|E_\theta| \leq |E_r|$. (9)

If $\rho = n\frac{\lambda}{\pi}\cos\theta$ then $|E_\theta| = n|E_r|$ (9a)

It is clear that at higher altitudes $|E_r| \geq \frac{1}{n}|E_\theta|$ on and inside at a semi-infinite cylinder of radius $\frac{n\lambda}{\pi}$. At any altitude:

$$\rho = z \tan\theta$$

so the surface on and inside of which $|E_r| \geq \frac{1}{n}|E_\theta|$ is:

$$z \tan\theta = n\frac{\lambda}{\pi}\cos\theta \qquad (10)$$

or

$$\tan\theta = \frac{n\lambda}{z\pi}\cos\theta \qquad (11)$$

This equation is plotted in Fig. 6 for $n = 0.1$, 0.2, and 1.0.

To summarize, the concept of a near and a far field on passes near or over the radio station is meaningless as far as the relative magnitudes of the various components are concerned. For this reason we will define that region in which the radial electric field E_r is appreciable relative to the transverse electric field, E_θ, as the "axial" field. We must recognize that it is not necessarily "near" the radiator but rather near the axis of the radiator and that it extends in a cylindrical form from above a few wavelengths vertically to infinity. Below a few wavelengths, it has the form depicted in Fig. 6. When θ approaches 90° it coincides with the near field.

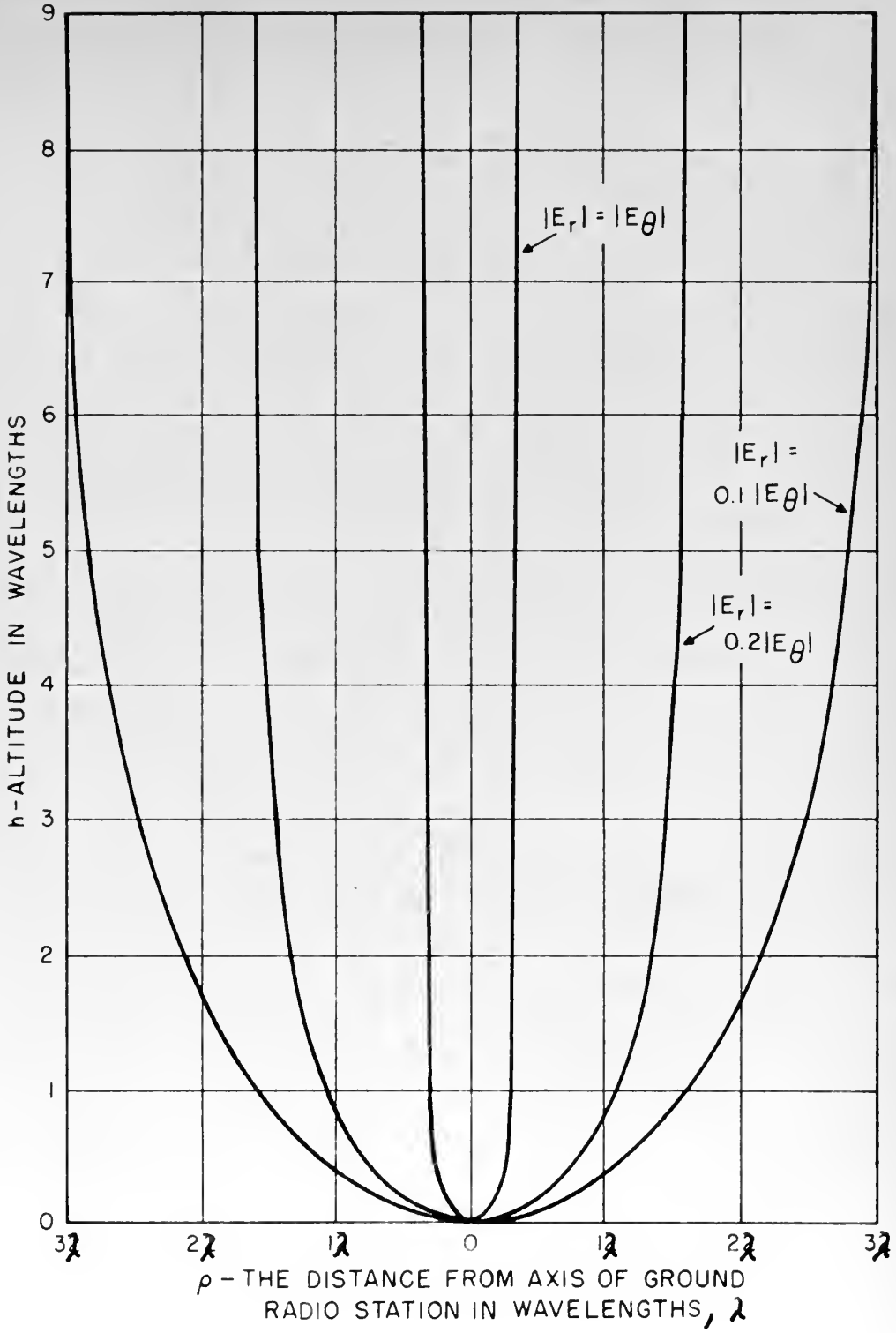

FIG 6

LINES OF CONSTANT $\left|\frac{E_r}{E_\theta}\right|$ OVER

VERTICAL ANTENNA ON GROUND

A-591-TR40-413

2. Derivation of Equation of Locus.

We have shown, in Fig. 5, the phase relations of the various field quantities. In Fig. 7 we see that the positive sense of E_θ induces a negative voltage component in the sense antenna before the "α" line passage, zero on the α line, and positive after the α line passage. Fig. 8 shows the phase relationships before the α line passage. A check of Figs. 9(a) and 9(b) indicates that some place between Fig. 9(a) and Fig. 9(b) the sense voltage will be in time quadrature with the shifted loop voltage. This is the point of sense antenna transition. If the phase shift, γ, were exactly $+90^\circ$ we can see that this point of phase quadrature would occur on the α line. In general γ is not exactly 90° and as a result the transition will in general occur either before or after the α line. At the quadrature point the loop will not be driven in either direction. This is the point of transition between a "stay where you are" signal and a "reverse your direction" signal to the needle (loop) while pointing to the station, or the point of transition between a "turn clockwise" and a "turn counter-clockwise" signal (or viceversa) to a loop not then steady on the bearing of the station. After this point of quadrature is passed, the loop will obey its new orders.

Thesis
W229

3 South Brunswick Avenue
Margate, New Jersey
August 1, 1955

Dear Professor Bauer,

While rewriting SRI Technical Report number 40 to appear in Transactions of the PGANE I found a few errors, mostly typographical. Except in the case of the correction to Figure 7, none of the corrections apply to the thesis as submitted to the school.

Will you please see that the thesis copies retained by the school are corrected as follows:

page 17, Fig. 7: make the angle "α" be measured from the "α line" to the vertical rather than to the horizontal.

Since returning to the East coast I have seen Mr. Clements in Norfolk and CDR Lawrence came up to Atlantic City to have me give him a flight in a TACAN equipped aircraft (AD-5N). I am the project officer on the TACAN Reliability project being carried on at VX-3.

My very best to Mrs. Bauer and to all.

Sincerely yours,

Herbert Ward

Herbert Ward

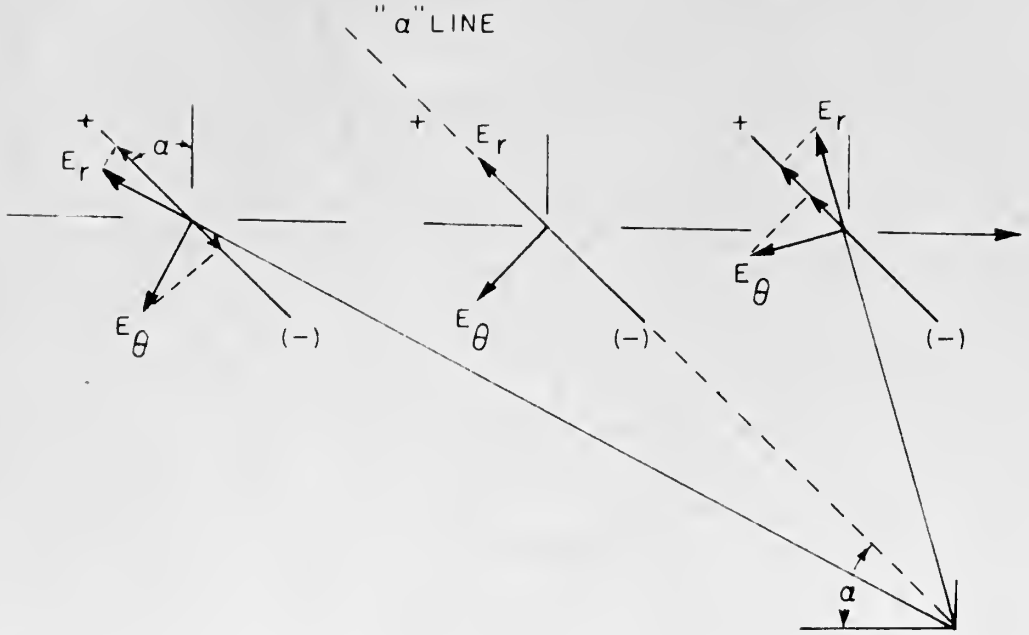

FIG. 7

THE SHIFT OF THE SENSE OF THE VOLTAGE COMPONENT IN THE SENSE ANTENNA DUE TO E_θ AS THE AIRCRAFT PASSES THE "α" LINE

A-591-TR40-414

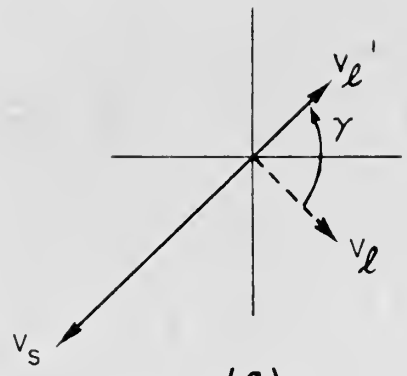

(a)

SPECIAL FAR FIELD
CASE WITH $\gamma = 90^\circ$

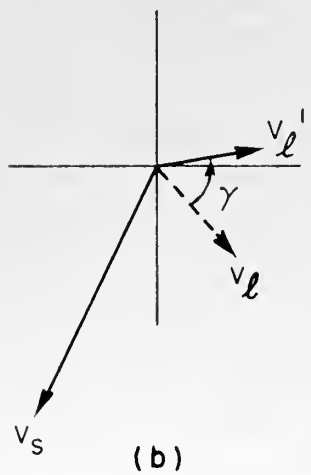

(b)

GENERAL CASE

FIG. 8

LOOP ANTENNA VOLTAGE ADVANCED γ° AND COMPARED WITH SENSE ANTENNA VOLTAGE BEFORE "a" LINE PASSAGE

A-591-TR40-415

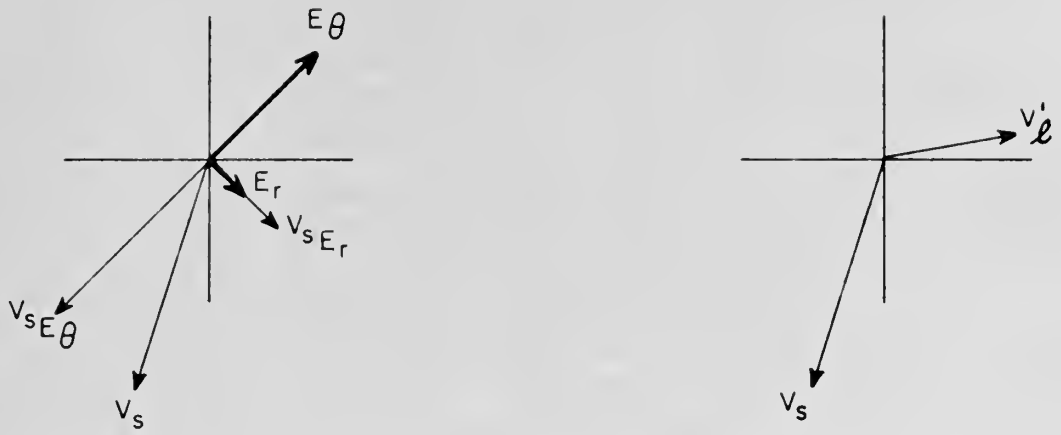

(a) BEFORE α LINE PASSAGE

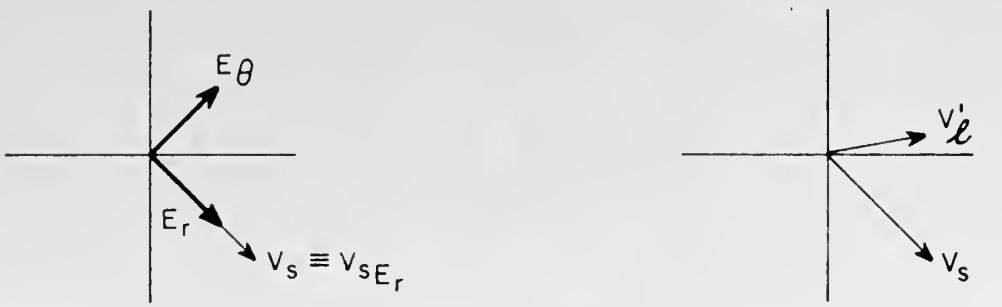

(b) ON α LINE

FIG. 9

CHANGE OF PHASE OF SENSE ANTENNA VOLTAGE RELATIVE TO LOOP VOLTAGE NEAR α LINE

A-591-TR40-416

As derived in Fig. 10, the point of sense transition will occur when the phase of the voltage in the sense antenna minus the phase of the H_ϕ field component equals the receiver phase shift minus 180°.

$$\angle V_s - \angle H_\phi = \gamma - 180^\circ \tag{12}$$

Consulting Fig. 4 where it is derived, the expression for the sense antenna voltage per unit length is:

$$V_s = E_z \cos\alpha + (E_\rho \cos\phi)\sin\alpha \tag{13}$$

where $E_\rho = E_r \sin\theta + E_\theta \cos\theta$

$E_z = E_r \cos\theta - E_\theta \sin\theta$

α = the effective tilt angle of the sense antenna.

Also on the ground plane of this figure we see that $\cos\phi = \frac{\sqrt{\rho^2 - d^2}}{\rho}$

Substituting equations (4) and (6) for E_θ and E_r :

$$E_\rho = \frac{\eta I_s}{2\pi r^2} U \cos\theta \sin\theta + j\frac{\eta I_s}{2\lambda r} U \sin\theta\cos\theta$$

$$= \frac{\eta I_s U}{2r}\left(\frac{1}{\pi r} + j\frac{1}{\lambda}\right)\sin\theta\cos\theta$$

$$E_z = \frac{\eta I_s}{2\pi r^2} U \cos\theta\cos\theta - j\frac{\eta I_s}{2\lambda r} U \sin\theta\sin\theta$$

$$= \frac{\eta I_s U}{2r}\left(\frac{\cos^2\theta}{\pi r} - j\frac{\sin^2\theta}{\lambda}\right)$$

using $\cos\phi = \frac{\sqrt{\rho^2 - d^2}}{\rho}$

$$V_s = \frac{\eta I_s U}{2r}\left(\frac{\cos^2\theta}{\pi r} - j\frac{\sin^2\theta}{\lambda}\right)\cos\alpha + \frac{\eta I_s U}{2r}\left(\frac{1}{\pi r} + j\frac{1}{\lambda}\right)\left(\frac{\sqrt{\rho^2 - d^2}}{\rho}\right)\sin\alpha\sin\theta\cos\theta \tag{13a}$$

$$V_s = \frac{\eta I_s U}{2r}\left[\left(\frac{\cos^2\theta\cos\alpha}{\pi r} + \frac{\sqrt{\rho^2 - d^2}}{\pi r\rho}\sin\theta\cos\theta\sin\alpha\right) + j\left(-\frac{\sin^2\theta\cos\alpha}{\lambda} + \frac{\sqrt{\rho^2 - d^2}}{\lambda\rho}\sin\theta\cos\theta\sin\alpha\right)\right] \tag{13b}$$

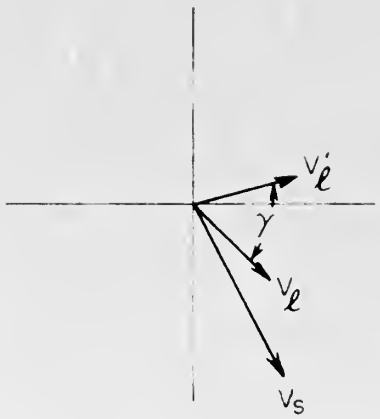

THERE WILL BE A POINT OF SENSE TRANSITION WHEN:

$$\angle V_\ell' - \angle V_S = 90$$

$$\angle V_\ell' = \angle H\phi - 90 + \gamma$$

$$\angle H\phi - 90 + \gamma - \angle V_S = 90$$

$$\angle H\phi - \angle V_S = 180 - \gamma$$

$$\angle V_S - \angle H\phi = \gamma - 180 \qquad (12)$$

FIG. 10

DEFINITION OF SENSE TRANSITION POINT

A-591-TR40-417

$$\angle V_s = \arctan \left[\frac{\frac{\sin\theta}{\lambda}\left(\frac{\sqrt{\rho^2-d^2}}{\rho}\cos\theta\sin\alpha - \sin\theta\cos\alpha\right)}{\frac{\cos\theta}{\pi r}\left(\frac{\sqrt{\rho^2-d^2}}{\rho}\sin\theta\sin\alpha + \cos\theta\cos\alpha\right)} \right] \quad (14)$$

$$= \arctan \left[\frac{\pi r}{\lambda} \tan\theta \frac{\left(\sqrt{\rho^2-d^2}\tan\alpha - \rho\tan\theta\right)}{\left(\sqrt{\rho^2-d^2}\tan\theta\tan\alpha + \rho\right)} \right] \quad (14a)$$

Again consulting Fig. 4(a) we see that $\tan\theta = \frac{\rho}{z}$ and $r = \sqrt{\rho^2+z^2}$ and therefore

$$\angle V_s = \arctan \left[\frac{\pi r \rho}{\lambda z} \frac{\left(\sqrt{\rho^2-d^2}\tan\alpha - \frac{\rho^2}{z}\right)}{\left(\frac{\sqrt{\rho^2-d^2}}{z}\tan\alpha + \rho\right)} \right] \quad (14b)$$

$$\tan\angle V_s = \left[\frac{\pi r}{\lambda z} \frac{\left(z\sqrt{\rho^2-d^2}\tan\alpha - \rho^2\right)}{\left(\sqrt{\rho^2-d^2}\tan\alpha + z\right)} \right] \quad (14c)$$

$$H_\phi = \frac{j I_s}{2\lambda r} U \sin\theta \quad (5)$$

and its phase is (+) 90°.

The point of sense transition will occur when

$$\angle V_s - \angle H_\phi = \gamma - 180^\circ \quad (12)$$

$$\angle V_s + 90^\circ = \gamma \quad (12a)$$

$$\tan\gamma = \tan(\angle V_s + 90) \quad (15)$$

$$\tan\gamma = -\cot\angle V_s \quad (15a)$$

From the above plus Eq. (14c) it is seen that

$$\tan\gamma = -\frac{\lambda z}{\pi r}\,\frac{\sqrt{\rho^2-d^2}\,\tan\alpha + z}{z\sqrt{\rho^2-d^2}\,\tan\alpha - \rho^2} \qquad (15b)$$

rearranging this and noting that $r = \sqrt{\rho^2+z^2}$ leads finally to the equation:

$$\sqrt{\rho^2-d^2} = \frac{\rho^2\pi\tan\gamma\sqrt{\rho^2+z^2} - \lambda z^2}{\pi\tan\gamma\tan\alpha\, z\sqrt{\rho^2+z^2} + \lambda z\tan\alpha} \qquad (16)$$

To summarize, it is seen with reference to Figs. 3 and 4 that the variables in this equation are:

ρ - the distance from the station to a point on the ground directly under the plane.

z - the altitude of the plane above the ground.

d - the distance that the flight path, projected vertically onto the ground, passes the station abeam.

γ - the total amount that the phase of the loop voltage is shifted toward the phase of the sense antenna signal by the receiver phase shifter and tuning circuits.

α - the tilt of the effective sense antenna of the aircraft relative to a vertical line through the aircraft.

A positive tilt angle is taken as a line from above the tail to below the nose, see Fig. 2.

λ - the wave length of the radio frequency signal.

To simplify the equation and to make the handling and consideration of the experimental data more meaningful, the linear dimensions of the equation will normally be expressed in wavelengths.

The normalized quantities are: $p = \frac{\rho}{\lambda}$, $h = \frac{z}{\lambda}$, and $b = \frac{d}{\lambda}$

and in normalized rotation, equ. 16 becomes

$$\sqrt{p^2 - b^2} = \frac{p^2 \pi \tan \gamma \sqrt{p^2+h^2} - h^2}{K \pi \tan \gamma \sqrt{p^2+h^2} + K} \qquad (16a)$$

where $K = h \tan \alpha$

This equation is that of a roughly paraboloidal surface oriented apex down. The traces of this surface on a vertical plane through the station in the direction of flight and on a horizontal plane a few wavelengths above the station are shown in Figs. 11 and 12.

It is to be remembered that the equation for this surface was derived as the locus of all points where the loop voltage and sense antenna voltages are 90° apart in time phase where they are combined in the receiver. At all points within this surface the ADF needle will tend to point away from the ground station (i.e., to assume a 180° bearing error) while at points outside of this surface the ADF needle will be driven toward the correct bearing.

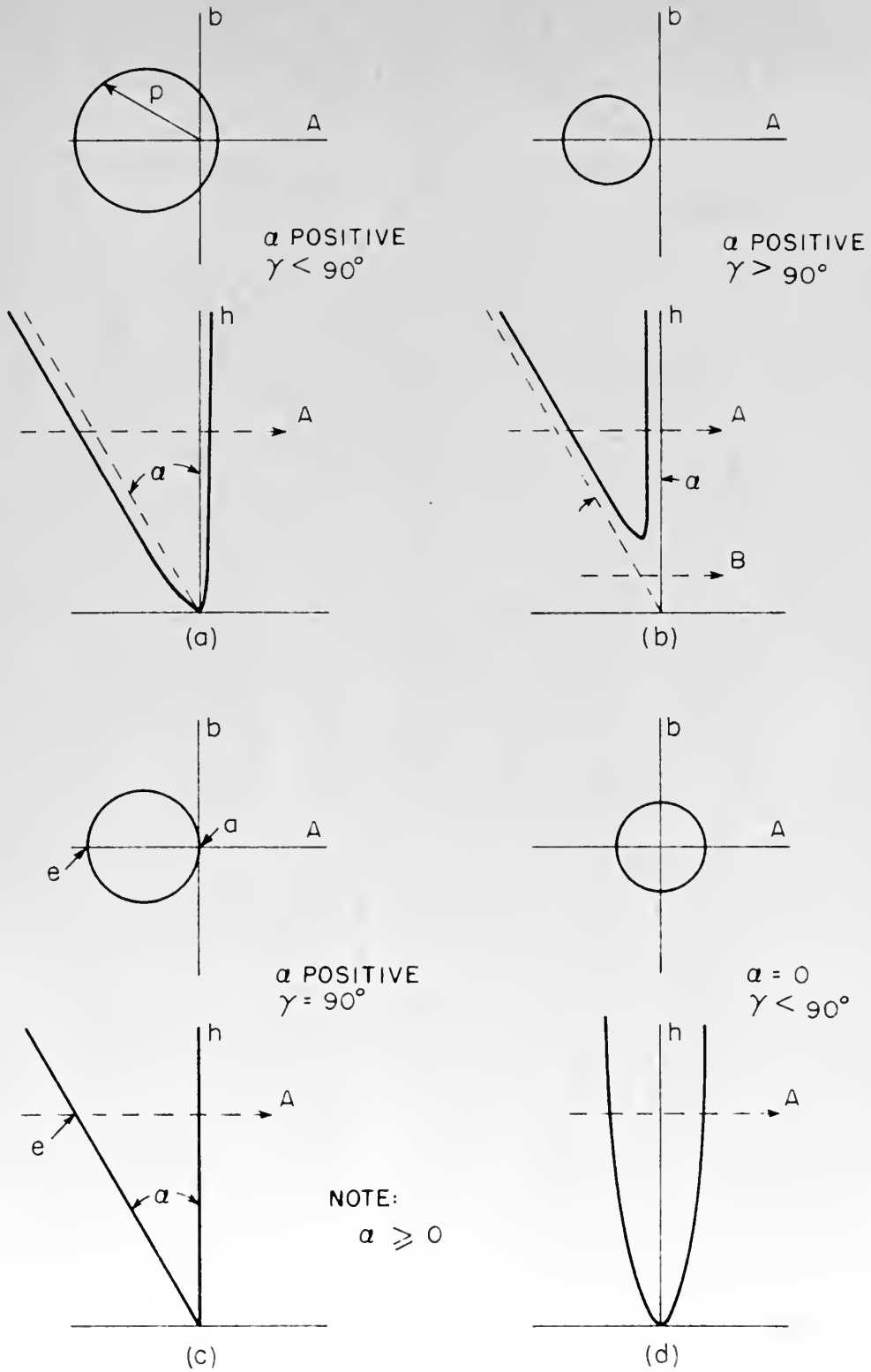

FIG. 11

SPACE FIGURE PLOTS OF EQUATION 16A

A-591-TR40-418

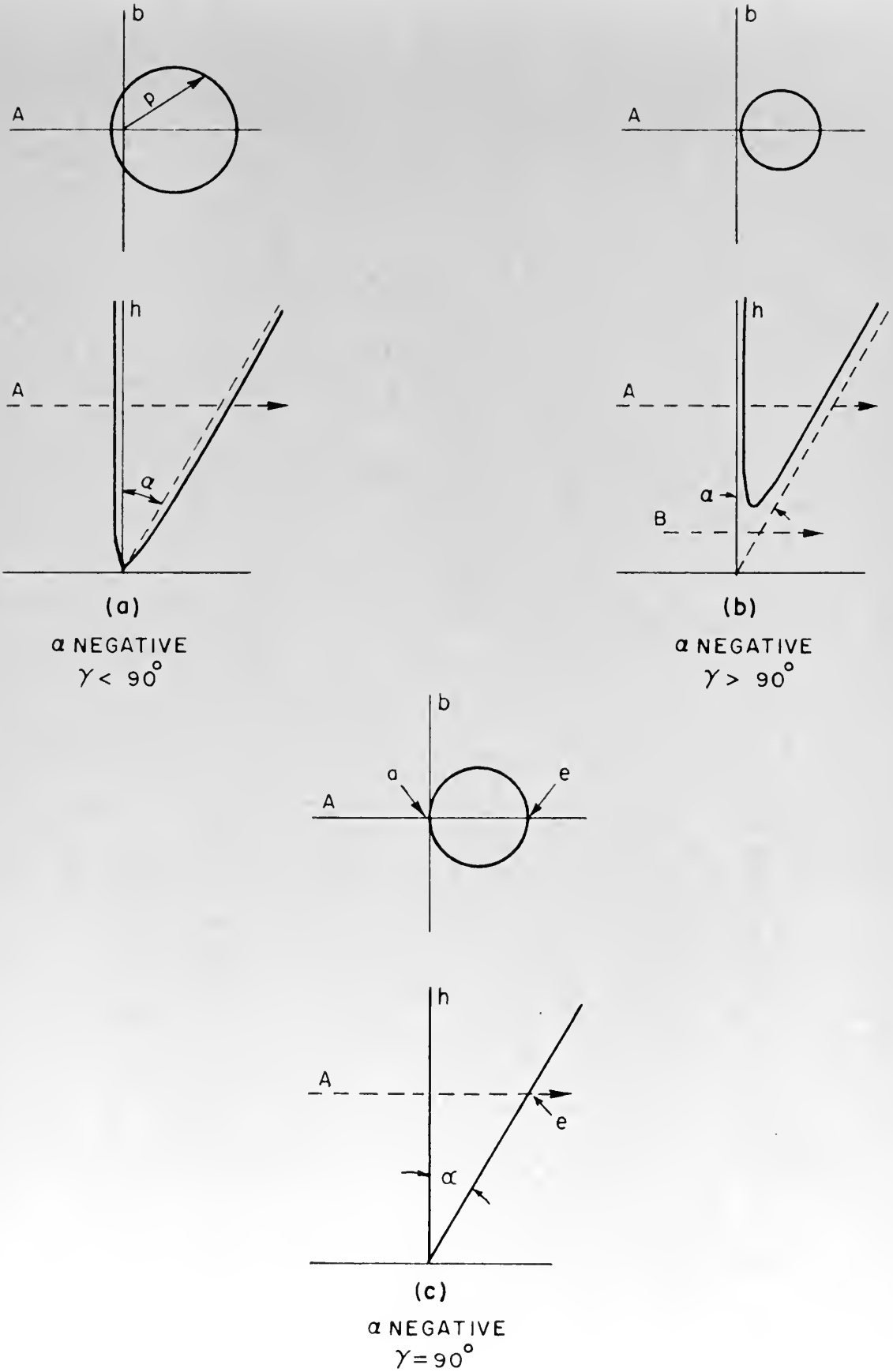

FIG. 12

SPACE FIGURE PLOTS OF EQUATION 16A

A-591-TR40-419

CHAPTER III

THE SPACE FIGURE

1. Investigation.

The equation derived in Chapter II is the locus of all points where the loop voltage and sense voltage are momentarily 90° apart when they are compared by the receiver. As this is the point of sense transition. Any time the airplane flys through this surface the needle of the radio compass indicator will start to reverse. Whether or not it will complete this reversal depends on whether or not it has enough time to completely reverse before another sense transition occurs.

There is one point of sense transition that is not shown by Eq.(16a). The equation gives the locus of the points of sense transition due to changes of the phase of the voltage in the sense antenna. When the aircraft passes the station there is a reversal of the loop or the loop signal due to the change in the direction of H_{ϕ} over the station. If the aircraft passes directly over the station, this loop phase transition is rapid as are the two sense antenna phase transitions. If the aircraft passes near the station but not over it, the loop phase transition will not occur as such but the loop will follow the gradual change of the direction in the normal manner.

To summarize, on any pass near or over the ground transmitting station, there will be in general three points where the ADF needle will tend to reverse, two sense antenna phase transitions and one loop phase transition. The order of occurrence and time spacing will be governed primarily by the speed and altitude of the plane, the phase shift of the receiver, the longitudinal location of the sense antenna (tilt angle) and the distance the plane passes abeam of the station axis.

There are four sets of conditions that will lead to only one compass reversal. First, if the aircraft misses the station wide enough so as not to fly through the space figure, the compass will continually point to the station axis and will reverse slowly as the plane passes. Second, if the flight path passes directly over the station axis and the receiver phase shift, γ, is exactly 90°, there will be one sense antenna transition and the loop transition right over the station. This corresponds to two rapid sense reversals simultaneously and will produce no effect. The only compass reversal in this case will be at the points marked "e" in Figs 11 (c) and 12(c), and will happen on the "α line" at a distance $h \tan \alpha$ before or after station passage respectively. Third, if the receiver phase shift, γ, is 90° and the tilt angle, α, is zero, corresponding to a vertical effective sense antenna, then we have a special case of the second case and the "α line" coincides with the vertical axis. In this case there will be one compass reversal. Lastly we have the case of Figs 11(b) and 12(b) where $\gamma > 90^{\circ}$. In this case the tip of the space figure rises off the ground. The greater the phase shift, the higher the tip. The smaller the tilt angle, the higher the tip. On any flight path such as "B" in these two figures, there will be only one compass reversal and it will occur on station passage.

As we would like the ADF to give a clear indication of station passage, the simple compass reversal is an attractive design objective. The first case considered above does not apply to flights directly over or near the station and hence is not available as a design variable. The second case produces a single reversal if $\gamma = 90^{\circ}$ but the compass reversal does not occur over the station so it does not meet the requirement.

The third case is ideal but it requires that " α " be exactly zero, necessitating a perhaps inconvenient longitudinal location of the sense antenna as well as centerline location. Furthermore, if this approach is used, the performance of the compass will vary with bank and trim. The fourth case requires only that the receiver phase shift be great enough and the antenna tilt small enough to raise the tip of the space figure above the altitude where the non-simple reversal would make any practical difference. With a phase shift of 110° and a tilt angle of $\pm 20^{\circ}$, the space figure tip would be 3.7 wavelengths above the ground. At 500 kc this would be 7280 feet. With a phase shift of 95° and a tilt angle of $\pm 10^{\circ}$ our limiting altitude would be 3.65 λ or 7180 feet at 500 kc. These are obviously above an altitude where split second accuracy is necessary.

On the following pages, Figs. 14 thru 21 illustrate the variation of the space figure with variation of the parameters. These figures were plotted directly from Eq. 16 (a). Fig. 13 is a conversion chart relating the altitude in wavelengths to the actual altitude and to the radio frequency. In all the two dimensional figures which follow, the linear dimensions are in wavelengths. Fig. 13 will assist in the practical interpretation of the curves.

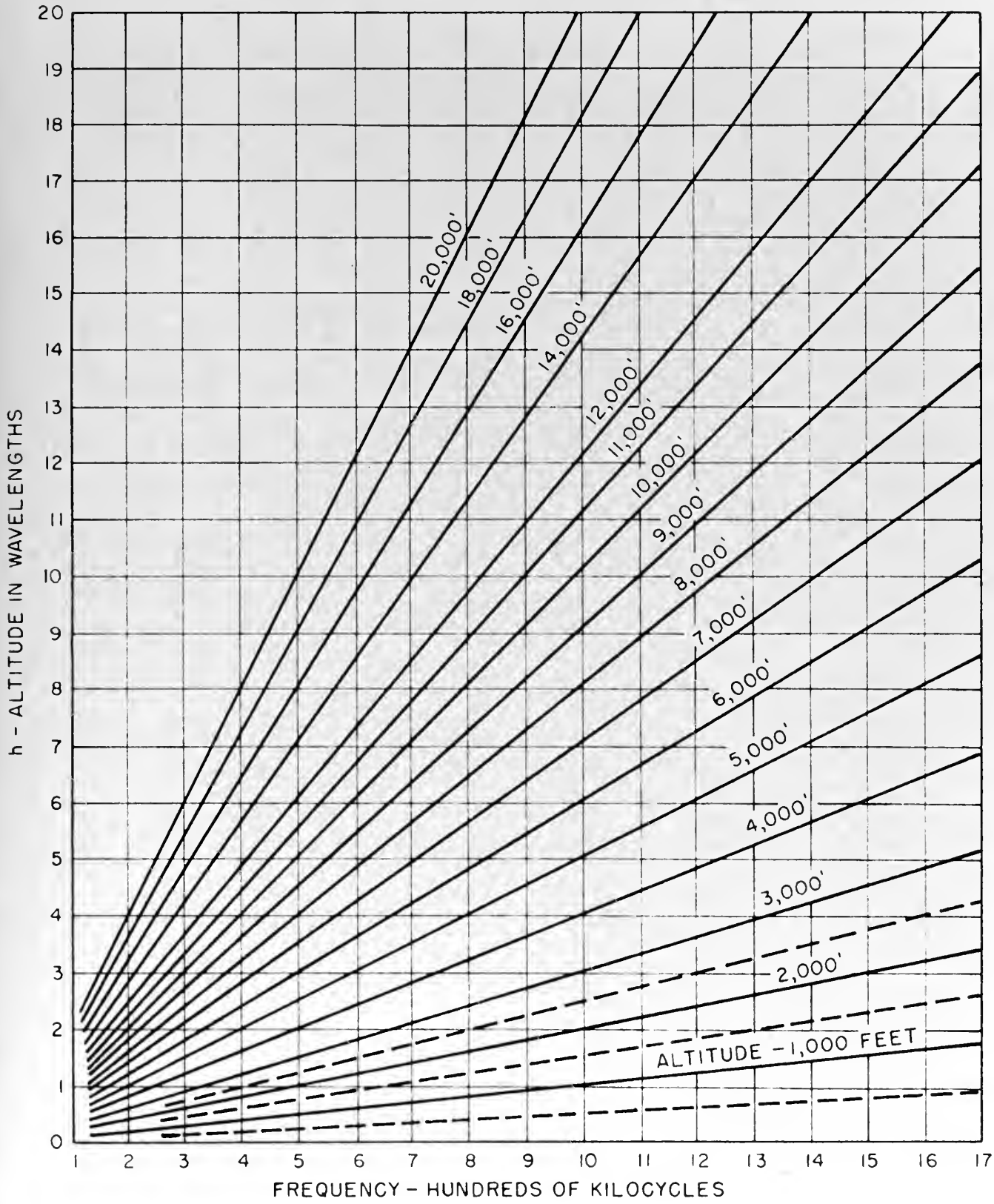

FIG. 13

CONVERSION CHART RELATING ALTITUDE IN WAVELENGTHS, h, TO ALTITUDE IN FEET

A-591-TR40-420

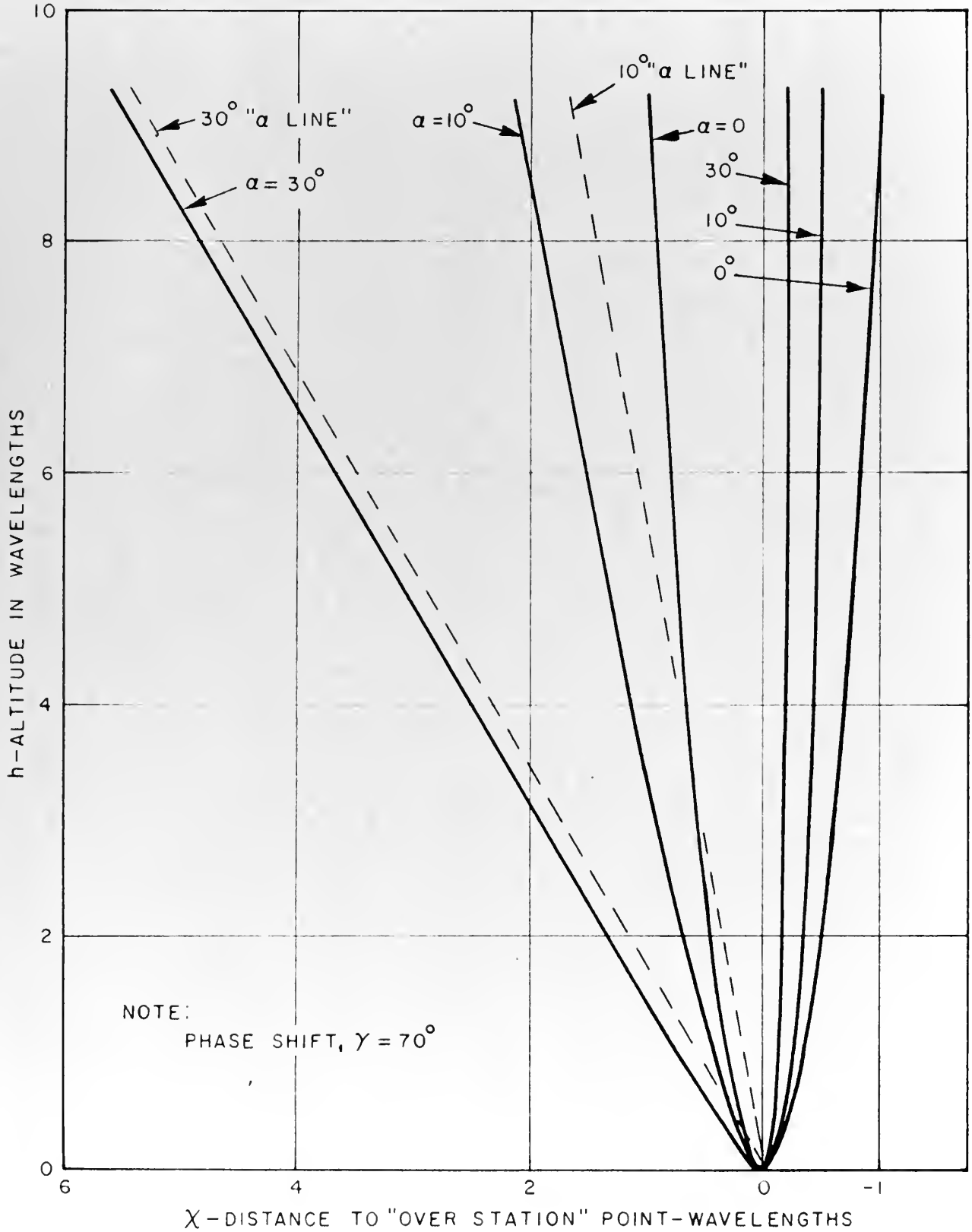

FIG. 14

VARIATION OF SPACE FIGURE WITH TILT ANGLE, α

A-591-TR40-421

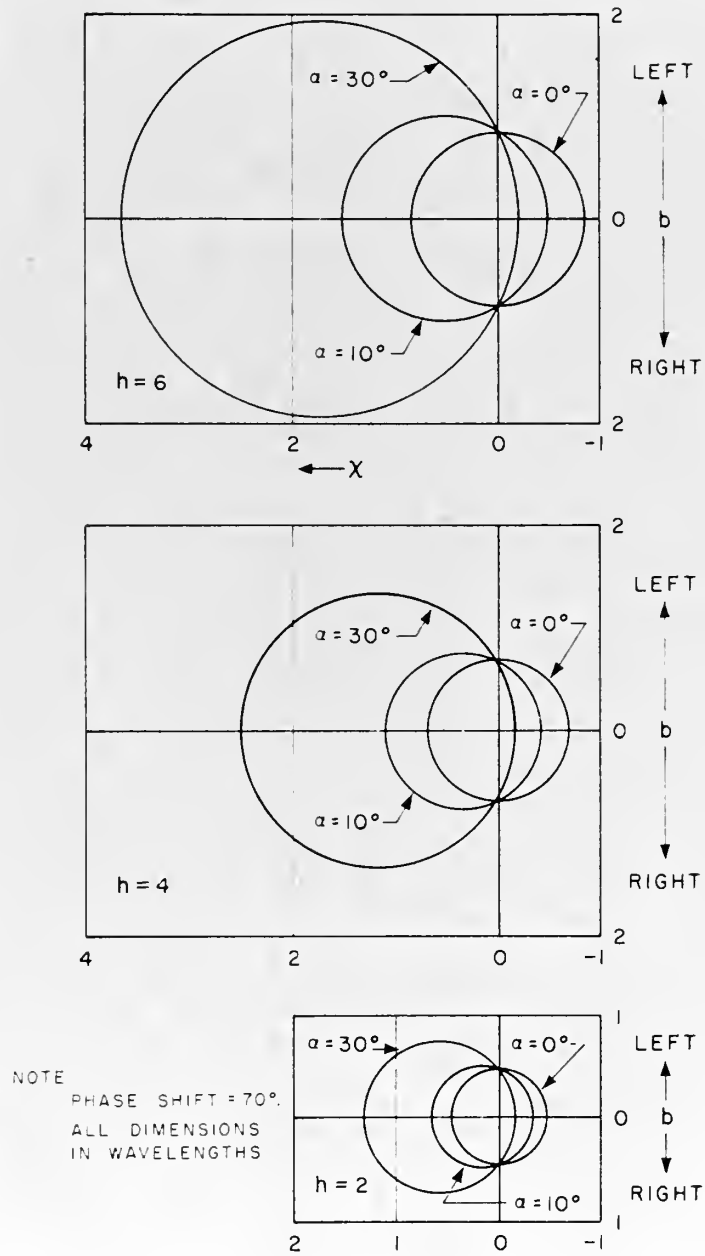

FIG. 15

HORIZONTAL SECTIONS OF FIG. 14 SHOWING VARIATION OF SPACE FIGURE WITH TILT ANGLE AND ALTITUDE.

B-591-TR40-422

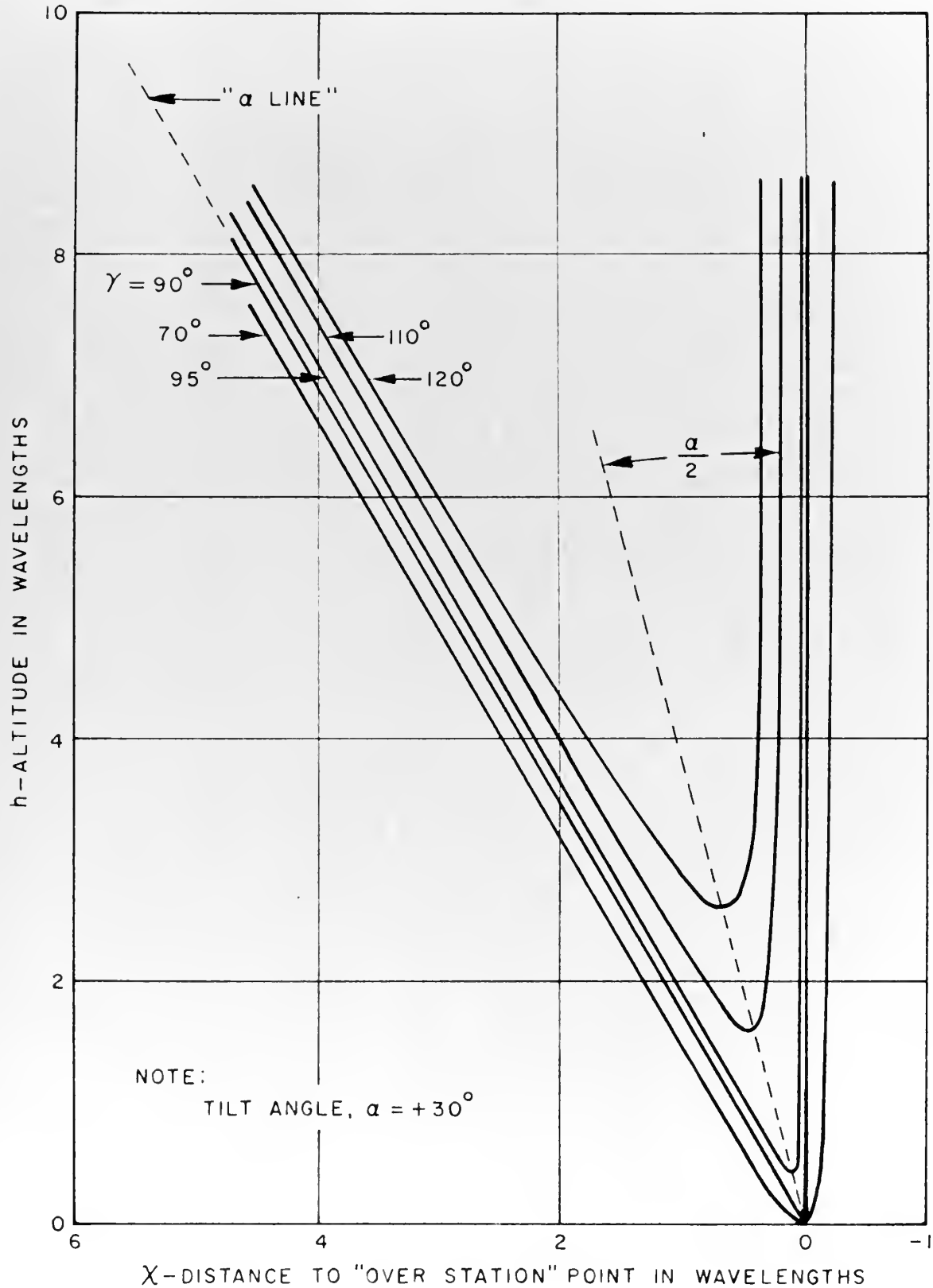

FIG. 16

VARIATION OF SPACE FIGURE WITH PHASE SHIFT, γ

A-591-TR40-423

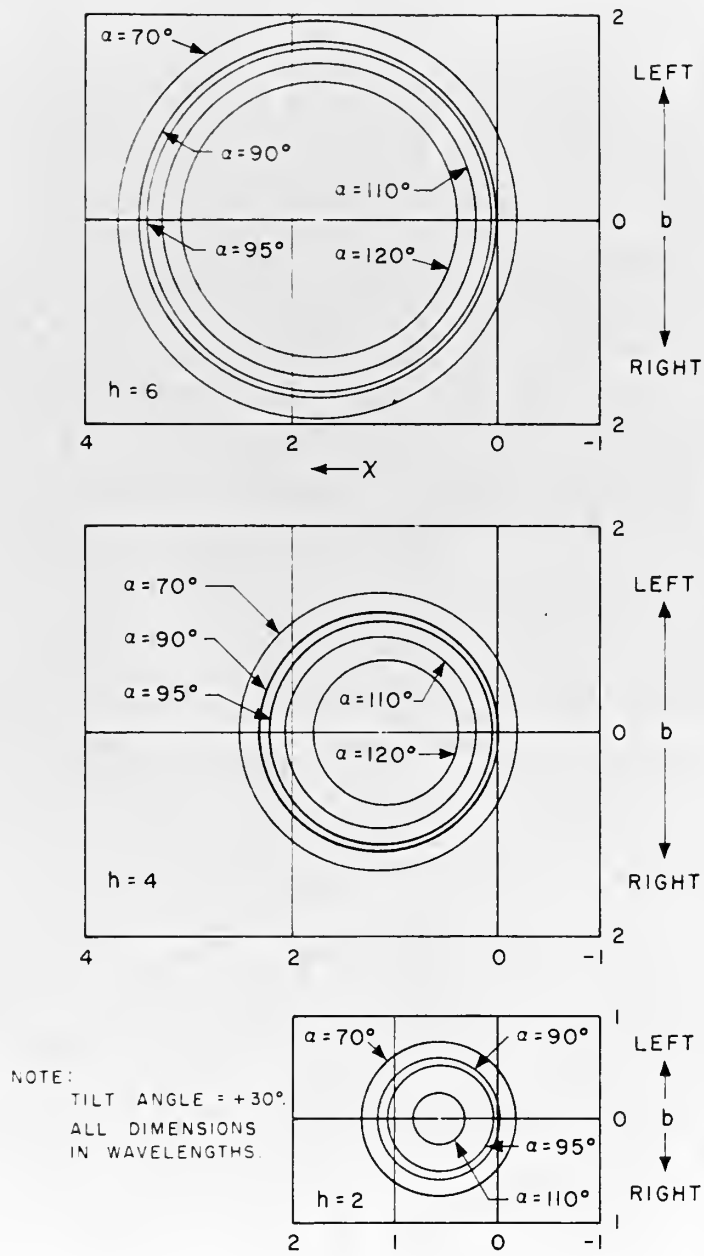

FIG. 17

HORIZONTAL SECTIONS OF FIG. 16 SHOWING VARIATION OF SPACE FIGURE WITH PHASE SHIFT AND ALTITUDE.

B-59:-TR40-424

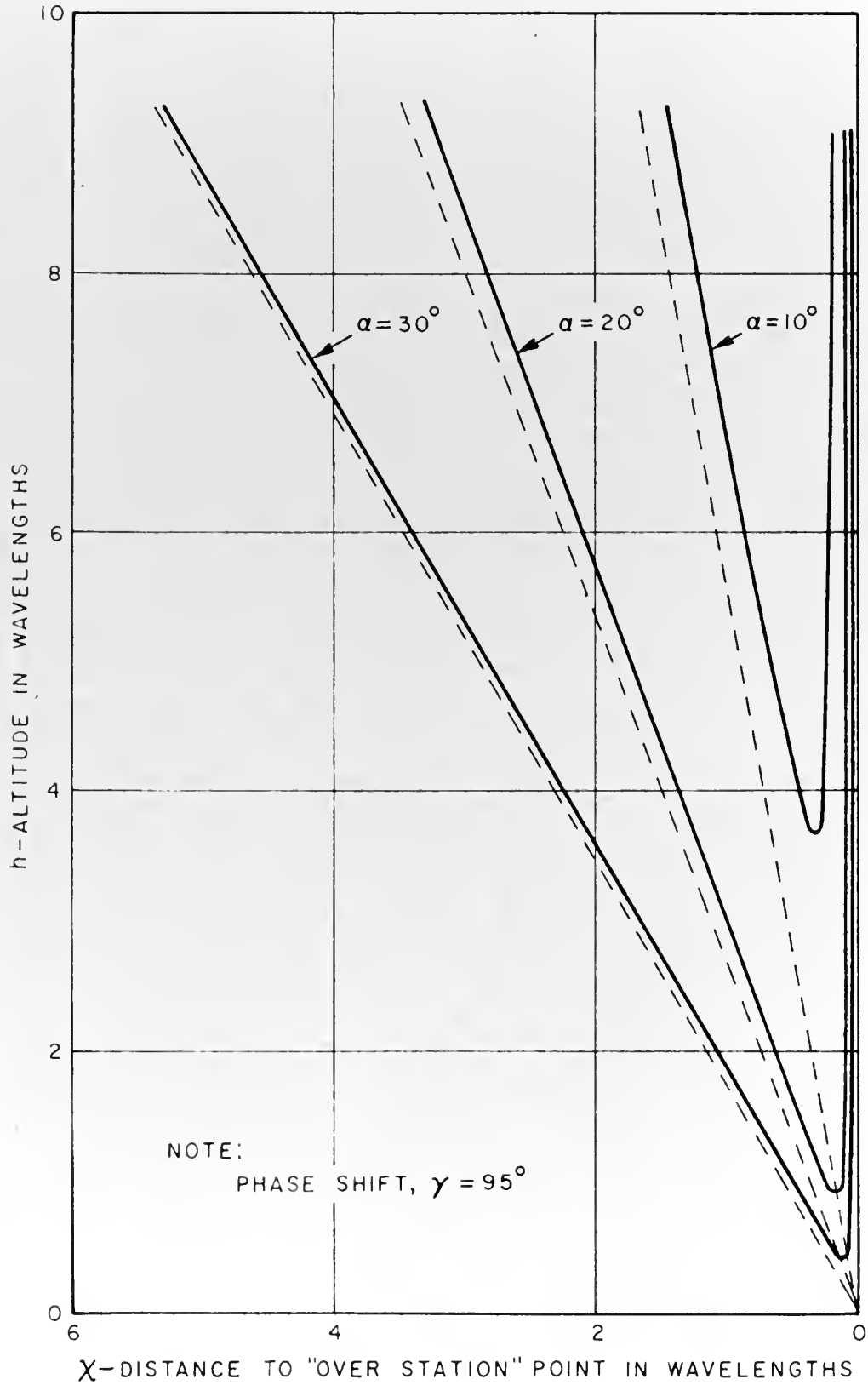

FIG. 18

VARIATION OF SPACE FIGURE WITH TILT ANGLE, α

A-591-TR40-425

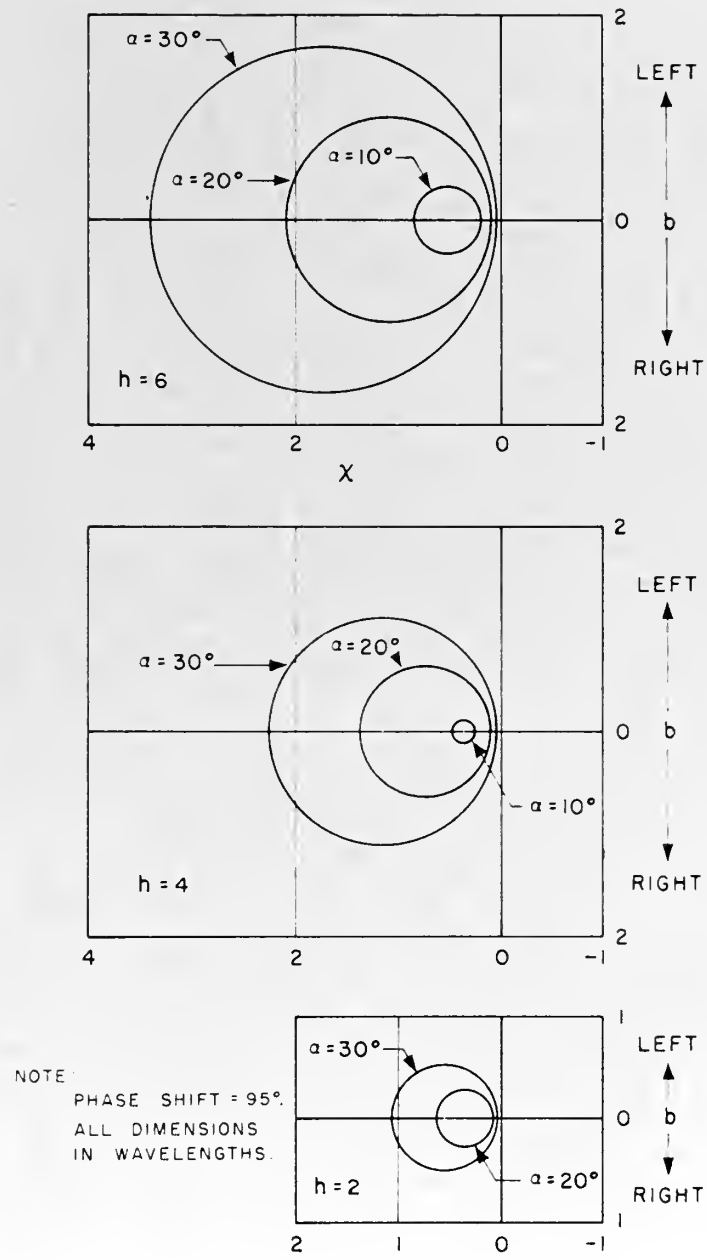

FIG. 19

HORIZONTAL SECTIONS OF FIG. 18 SHOWING VARIATION OF SPACE FIGURE WITH TILT ANGLE AND ALTITUDE.

B-591-TR40-426

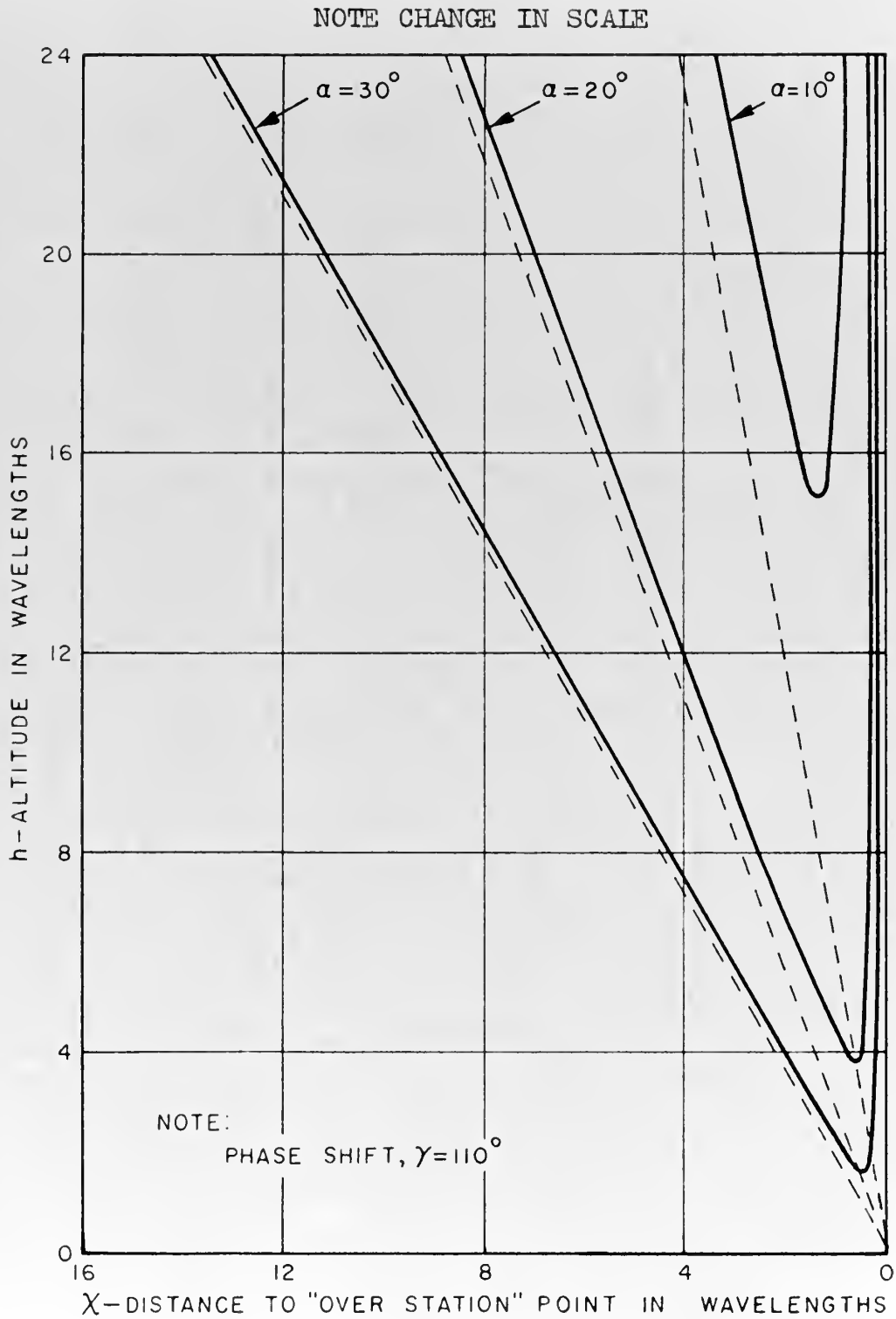

FIG. 20

VARIATION OF SPACE FIGURE WITH TILT ANGLE, α

A-591-TR40-427

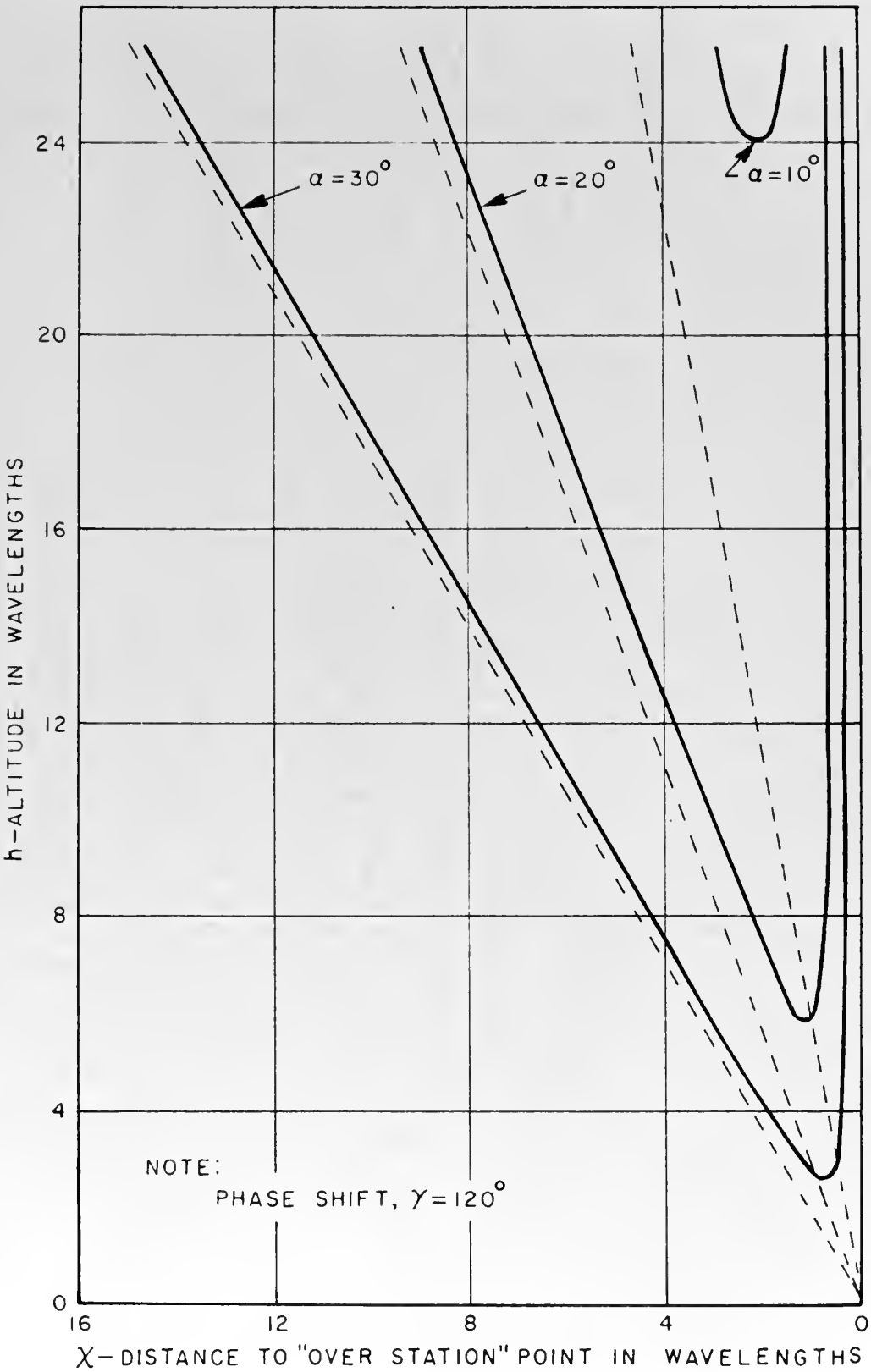

FIG. 21

VARIATION OF SPACE FIGURE WITH TILT ANGLE, α

A-591-TR40-428

2. The altitude of Space Figure Tip.

It would be convenient to have a formula for computing the altitude of the tip of the space figure without the elaborate computing and plotting technique used in obtaining the eight preceding figures. At one step in the derivation of the space figure equation we had

$$\tan\gamma = -\frac{\lambda z}{\pi r}\,\frac{\sqrt{\rho^2-d^2}\tan\alpha + z}{z\sqrt{\rho^2-d^2}\tan\alpha - \rho^2} \qquad (15b)$$

Starting with this equation we may derive an expression giving the height of the space figure tip directly in terms of γ and α .

As the tip falls above the " x " axis (b= 0), we may replace ρ by $x\lambda$ and then normalize, replacing z by h , and λ by 1, and r by n to give:

$$\tan\gamma = \frac{h}{\pi n}\,\frac{x\tan\alpha + h}{x^2 - hx\tan\alpha} \qquad (15c)$$

Setting $\pi\tan\gamma = A$ and rearranging,

$$An x^2 - (An+1)h\tan\alpha\, x - h^2 = 0$$

for x to be real

$$\left[(An+1)h\tan\alpha\right]^2 + 4An h^2 \geqslant 0 \qquad (17)$$

This will be satisfied for any h if $0 < \gamma < 90^\circ$ so that A is positive. We will then have a space figure whose tip touches the ground.

When $90^\circ < \gamma < 180^\circ$, as we have seen, the tip rises from the ground. At the tip x must be single valued:

$$(An+1)^2\tan^2\alpha = -4An \qquad (17a)$$

Solving this for n ,

$$n = (-)\,\frac{(\sec\alpha+1)^2}{A\tan^2\alpha} \qquad (18)$$

Now ℓ is actually equal to $\sqrt{x^2 + h^2}$. It is noted from Fig. 16 that the tip falls very near the line $\frac{\alpha}{2}$, and we may set $\ell = \sqrt{x^2+h^2} = h \sec \frac{\alpha}{2}$. This gives the expression desired

$$h = (-) \frac{(\sec \alpha + 1)^2}{\pi \tan \gamma \tan^2 \alpha \sec \frac{\alpha}{2}} \tag{19}$$

This further reduces to the simpler form

$$h = (-) \frac{\cos \frac{\alpha}{2}}{\pi \tan \gamma \tan^2 \frac{\alpha}{2}} \tag{19a}$$

We can now plot γ vs α with the altitude of the space figure tip, h, as a perameter. Such a plot is shown in Fig. 22. From the figure we may determine what receiver phase shift, γ, would be required to produce single compass reversals on all station passages below a specified altitude, h, with an aircraft whose tilt angle is α.

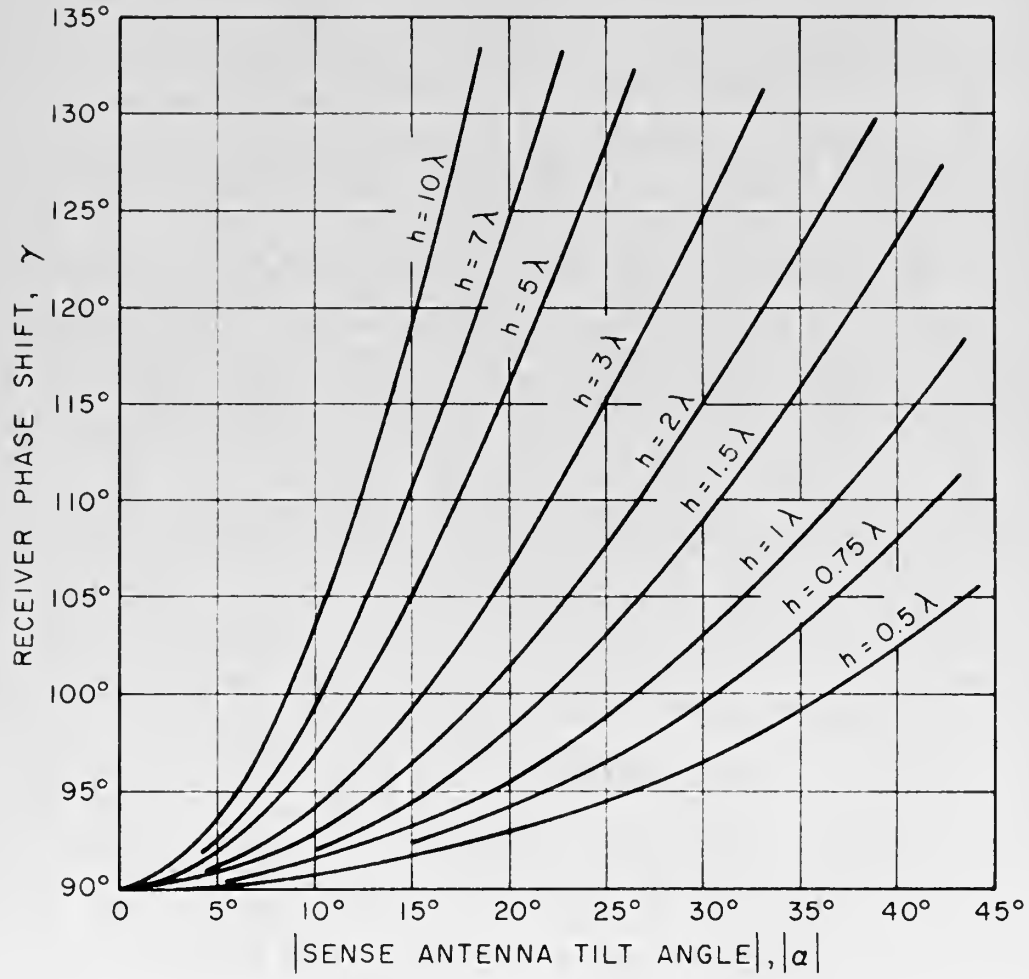

NOTE: PLOTTED FROM:

$$h = (-)\frac{\cos\frac{\alpha}{2}}{\pi \tan\gamma \tan^2\frac{\alpha}{2}} \quad \text{(EQ. 19a)}$$

FIG. 22

PHASE SHIFT AND TILT ANGLE REQUIRED TO PLACE THE LOWER TIP OF THE SPACE FIGURE AT AN ALTITUDE h-WAVELENGTHS

A-591-TR40-429

3. The Asymptotes of the Space Figure.

It appears from the plotted vertical sections of the space figure (Figs. 14, 16 and 18) that the two legs of the curves are not asymptotic to the α line and the h axis respectively but seem to be asymptotic to lines at constant distances from these lines. As shown in Chapter II (1) the E_θ and E_r fields are of the same order of magnitude in a cylindrical region above the ground station. Consider an aircraft on a flight path passing from left to right directly over the station and consider the vertical section containing the flight path of the aircraft, $\rho \equiv |x|$ with the convention that x is positive to the left of the station. Eq. (16a) now becomes,

$$X = \frac{x^2 \pi \tan\gamma \sqrt{x^2+h^2} - h^2}{h \tan\alpha (\pi \tan\gamma \sqrt{x^2+h^2} + 1)} \qquad (20)$$

Setting up the following conditions which are compatible with the practical problem: $45^\circ < \gamma < 135^\circ$,

$$-60^\circ < \alpha < 60^\circ ,$$

letting $\pi \tan\gamma = A$, and noting that in the asymptotic region h will be very large so that

$$A\sqrt{x^2+h^2} + 1 \approx A\sqrt{x^2+h^2}$$

we have

$$x = \frac{x^2 A \sqrt{x^2+h^2} - h^2}{h A \tan\alpha \sqrt{x^2+h^2}} \qquad (20a)$$

for all practical purposes in the asymptotic region.

The main difficulty in the investigation of this expression is the radical $\sqrt{x^2+h^2}$. For the leg of the curve which nearly parallels the h axis we have $x \ll h$ in the asymptotic region.

Then the radical $\approx h$ and we have

$$X = \frac{x^2 A - h}{A h \tan\alpha} = \frac{x^2 - \frac{h}{A}}{h \tan\alpha}$$

or

$$x^2 - (h \tan\alpha)x - \frac{h}{A} = 0$$

the roots of which are

$$X = \frac{h \tan\alpha}{2}\left(1 \pm \sqrt{1 + \frac{4}{h A \tan^2\alpha}}\right) \qquad (21)$$

We are investigating the leg near the h axis. The positive radical would give an answer of the order of $h \tan\alpha$ which is along the α line where the approximation does not hold. Therefore, only the negative radical is retained in Eq.(21).

In the asymptotic region, provided that α is not small, the second term under the radical is much smaller than unity and

$$X = \frac{h \tan\alpha}{2}\left(1 - 1 - \frac{2}{h A \tan^2\alpha}\right)$$

$$X = -\frac{1}{A \tan\alpha} \equiv -\frac{1}{\pi \tan\gamma \tan\alpha} \qquad (21a)$$

This equation states that the asymptote: (1) is a function of only γ and α, (2) is closer to the h axis the nearer γ is to 90° and the larger the tilt angle, (3) is to the left of the h axis for $\gamma > 90^\circ$, to the right for $\gamma < 90^\circ$. See Figs. 16 and 18.

If $\alpha \approx 0$

$$X = -\sqrt{\frac{h}{A}},$$

a parabola as shown in Fig. 14.

Proceeding similarly to investigate the other leg of the vertical section, near the α line X is no longer small relative to h. However, $X \approx h \tan\alpha$

$$\sqrt{x^2 + h^2} \approx h\sqrt{1 + \tan^2\alpha} = h \sec\alpha$$

Again proceeding from Eq. (20a) we have

$$X = \frac{X^2 A h \sec\alpha - h^2}{h^2 A \tan\alpha \sec\alpha}$$

the roots of which are

$$X = \frac{h \tan\alpha}{2}\left(1 \pm \sqrt{1 + \frac{4}{Ah \tan^2\alpha \sec\alpha}}\right) \quad (22)$$

In this case we are interested in the root $X \approx h \tan\alpha$ so we must chose the plus sign.

In the asymptotic region, provided that α is not too small, the second term under the radical is much smaller than unity and

$$X = \frac{h \tan\alpha}{2}\left(1 + 1 + \frac{2}{h \tan^2\alpha \sec\alpha \pi \tan\gamma}\right)$$

$$X = h \tan\alpha + \frac{\cos\alpha}{\pi \tan\gamma \tan\alpha} \quad (22a)$$

This equation shows that the asymptote;(1) is parallel to $h \tan\alpha$, the α line, (2) is horizontally spaced from the α line by a constant amount $\frac{\cos\alpha}{\pi \tan\gamma \tan\alpha}$

(3) is below the α line if $\gamma < 90°$, above it if $\gamma > 90°$,

(4) is coinciding with the α line when $\gamma = 90°$,

(5) is close to the α line for γ near $90°$ and for larger α.

See Figs. 16 and 18.

If $\alpha \approx 0$

$$X = \sqrt{\frac{h}{A \sec\alpha}} = \sqrt{\frac{h}{A}}$$

the other leg of the parabola, see Fig. 14.

In the event that we have a negative α, we have the situations of Fig. 12 instead of Fig. 11, and the two expressions for the asymptotes are still valid and in accordance with our sign convention.

CHAPTER IV

FLIGHT TESTING

1. Test Equipment Development.

A total of five test flights were made to verify the results of the preceding theoretical investigation. The first flight was made during the first week of the project to examine critically the performance of the radio compass at various altitudes over a variety of types of stations at various frequencies. After this flight, although as a pilot the writer had noticed the erratic performance of the ADF many times and taken it for granted, he was thoroughly impressed with the actual gyrations of the needle.

It was obvious that some quantity would have to be recorded to be studied and analyzed. Although the actual compass needle motion could be recorded either photographically or electrically it was decided that a greater insight into the actual signal could be gained by placing the loop in a fixed position, namely with the axis pointing 90° to the left or right, and then recording the output of the servo amplifier as it tried to drive the loop toward the zero loop signal position. This method would give the instantaneous result not hampered by the long time constant of the loop drive system.

A study of the circuit diagram shows that the direction of the loop motion is controlled by the phase of the control winding voltage relative to the phase of the reference winding voltage supplied to the loop drive two phase induction motor. This phase is in turn determined by which of two voltages, 180° out of phase with each other and each 90° to the reference voltage, predominates in the control winding voltage to the loop motor. Fig. 23 shows the simplified functional arrangement.

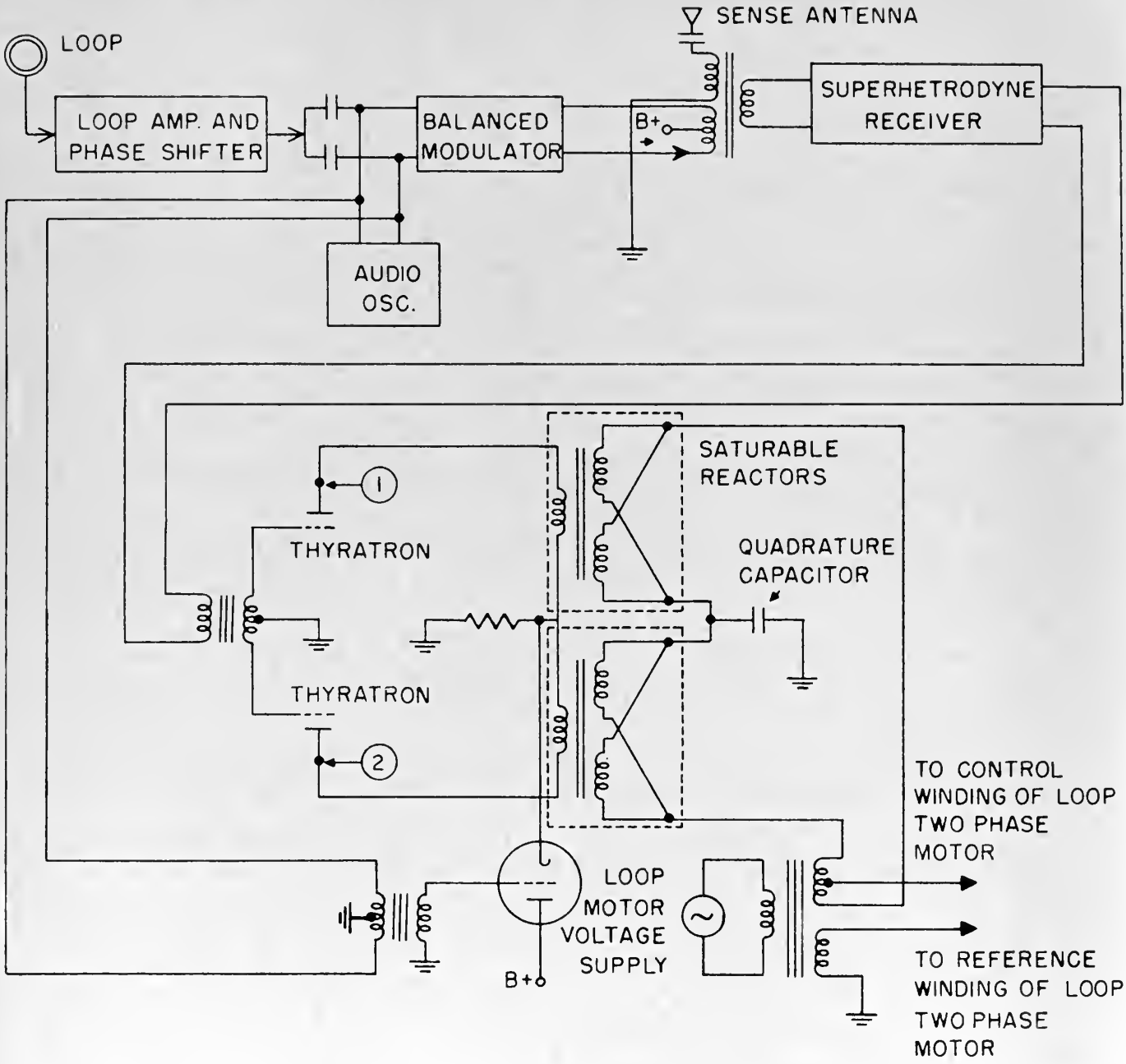

FIG. 23

FUNCTIONAL DIAGRAM OF ARN-7 WITH FUNCTION SWITCH ON "COMPASS"

A-591-TR40-430

The outputs of the two thyratrons feed through two saturable reactors. The plates of the thyratrons are driven through a cathode follower at an audio rate and in phase by an audio oscillator in the receiver. This same oscillator drives a balanced modulator modulating the R. F. input from the loop after it has been amplified and shifted ahead γ° in phase. The output of the balanced modulator is added to the sense antenna signal and the sum is applied to the input of a superheterodyne receiver. The input to the receiver section is therefore modulated at the audio rate. The phase of this modulation depends on the phase relation between the sense antenna voltage and the shifted loop antenna voltage. The demodulated output from the second detector of the receiver is fed push-pull to the grids of the thyratrons. The grids are thereby driven 180° out of phase; and one grid, depending on the phase of the modulation on the signal applied to the superheterodyne receiver section above, is in phase with its plate. This tube conducts each cycle while the other does not conduct. This conduction current saturates the saturable reactor associated with that thyratron and the reactor acts as a switch passing current to the control winding of the loop induction motor. The cathode follower supplies the audio signal superimposed on a d.c. value. The d.c. potential of the plate of the thyratron which is conducting will be lower than that of the other plate. To determine the points of sense transition, viz. the point where the loop stops being driven one way, say toward the nose, and starts being driven toward the tail of the aircraft, we have only to record the change in the d.c. potentials of the two plates. More exactly, it was decided to record the magnitude and polarity of the difference in d.c. level between the plates.

The circuit shown in Fig. 24 was built and tested on an NA-1 unit in the screened room. The ultimate design was to be used on various types of

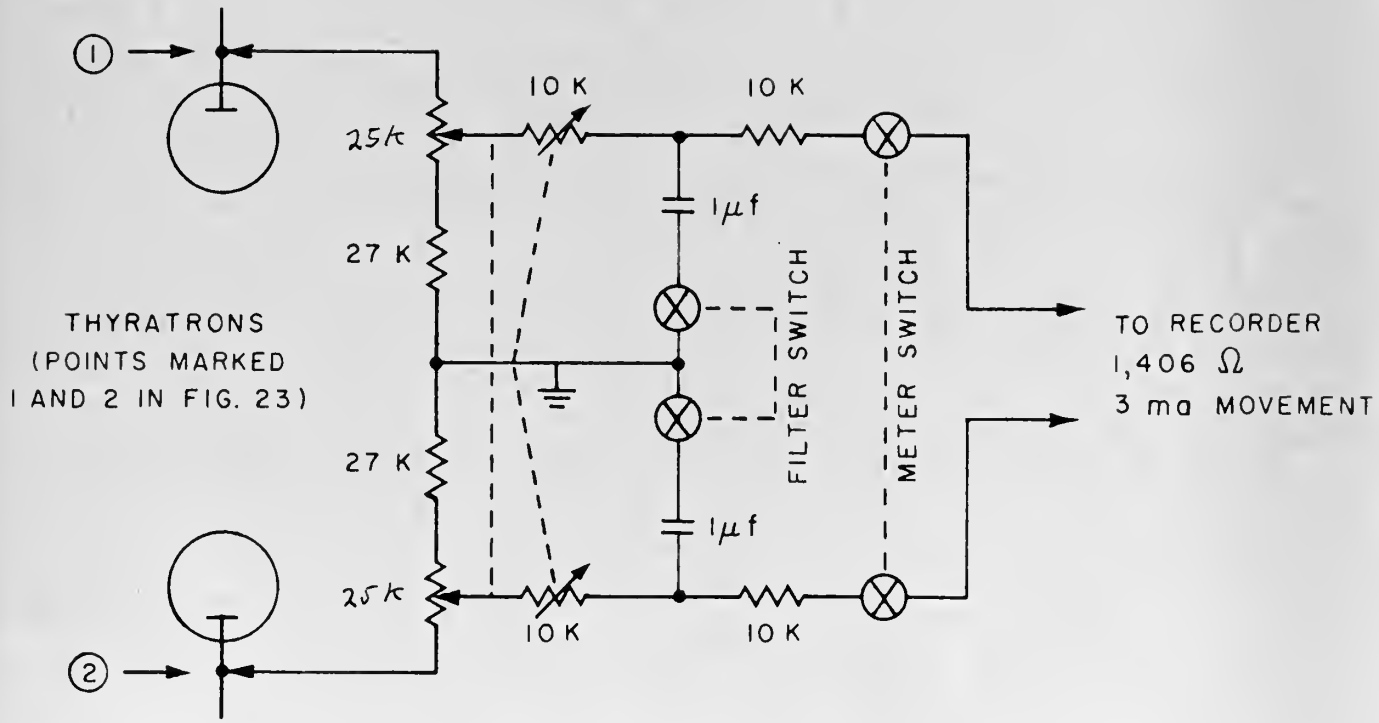

FIG. 24

RECORDER ATTENUATOR CIRCUIT

A-591-TR40-431

units in several different aircraft. As no modifications of the ADF receivers in these aircraft could be made, all connections had to be plug-in or clip types; and the receiver had to remain in its rack in an operating condition. The easiest way to pick off the plate potentials of the thyratrons was to use two new type 2050 tubes and solder wires to the plate pins. These 2050's were then placed in the set in place of those installed. The recording system seemed to operate satisfactorily, and it was then flight tested in test "A". The flight test proved the system operable.

Flight test "B" was run making passes over stations of various frequencies and at various altitudes. These runs were made at altitudes from h=0.6 to h = 10. The test showed in general the three predicted points of sense transition, two due to the sense antenna transition and one due to the loop transition. At certain headings over the tower of KMBY in Monterey the signal level seemed to vary in a regular manner with several maxima and minima after the station passage. The tower is located on the end of a very long pier which carries water pipes, power lines, and similar conductors to its outer end. It is felt that these elements caused the interference pattern noted. This test showed that the tilt angle of this aircraft, an SNB-5, was about (-) 37°. The sense antenna is below the aircraft and astern of the wings so that the observed tilt direction was consistent with that expected.[6] It also showed that the recorder system would function very well with the SCR 269-F(BC-433 F) which uses 6SK7's instead of 2050's as the control tubes. The system of making the servo amplifier phase sensitive is slightly different but the results are the same as far as the 6SK7's d.c. plate level variations are concerned, and the recording system is suitable for both types. When the 6SK7's are used the trace is smooth as shown on the recording in Fig.31

even with the filter turned off. When the ADF being used for the test uses 2050's or 2051's the trace is rough as shown in Figs 33 and 34 even with the filter cut on. With the filter off, the results are completely unusable.

During test "B" three runs were made at h = 2.9 over MRY, the homer at Monterey (356 KC). For the first run the receiver was tuned for maximum signal, 357.5 on the dial. A single transition was noted. The second run was made with the receiver tuned to 359. Again a single transition was noted. The third run was made with the receiver tuned low, to 352. This time the three transition pattern was found. Upon analysis this lead to the conjecture that tuning high produced a phase shift greater than 90° and tuning low made γ less than 90°. This could account for some of the unreproducibility of data on seemingly similar runs reported by other investigators. It also stands to reason, because the phase of the current in a tank circuit driven by a fixed frequency is certainly a definite function of the tuning of the tank circuit.

It was obvious that the one quantity in Eq. (16a) over which we had no control was γ, the total receiver phase shift up to the mixing point.

A phase shifter was designed and built. The circuit is shown in Fig. 25 and photographs of the actual equipment are shown in Figs. 26 and 27. The phase shifter was calibrated at frequencies of 203, 356, 388, 414, and 680 KC's, all being frequencies of available stations in the area. Calibration curves, of which Fig. 28 is an example, were constructed at each frequency. The gain of the completed circuit at various frequencies is shown in the following table:

Frequency	Maximum Gain	Minimum Gain
203 Kc	14.8 db	14.0db
356 Kc	12.9 db	12.7db
414 Kc	8.0 db	7.6db
680 Kc	7.2 db	5.6db

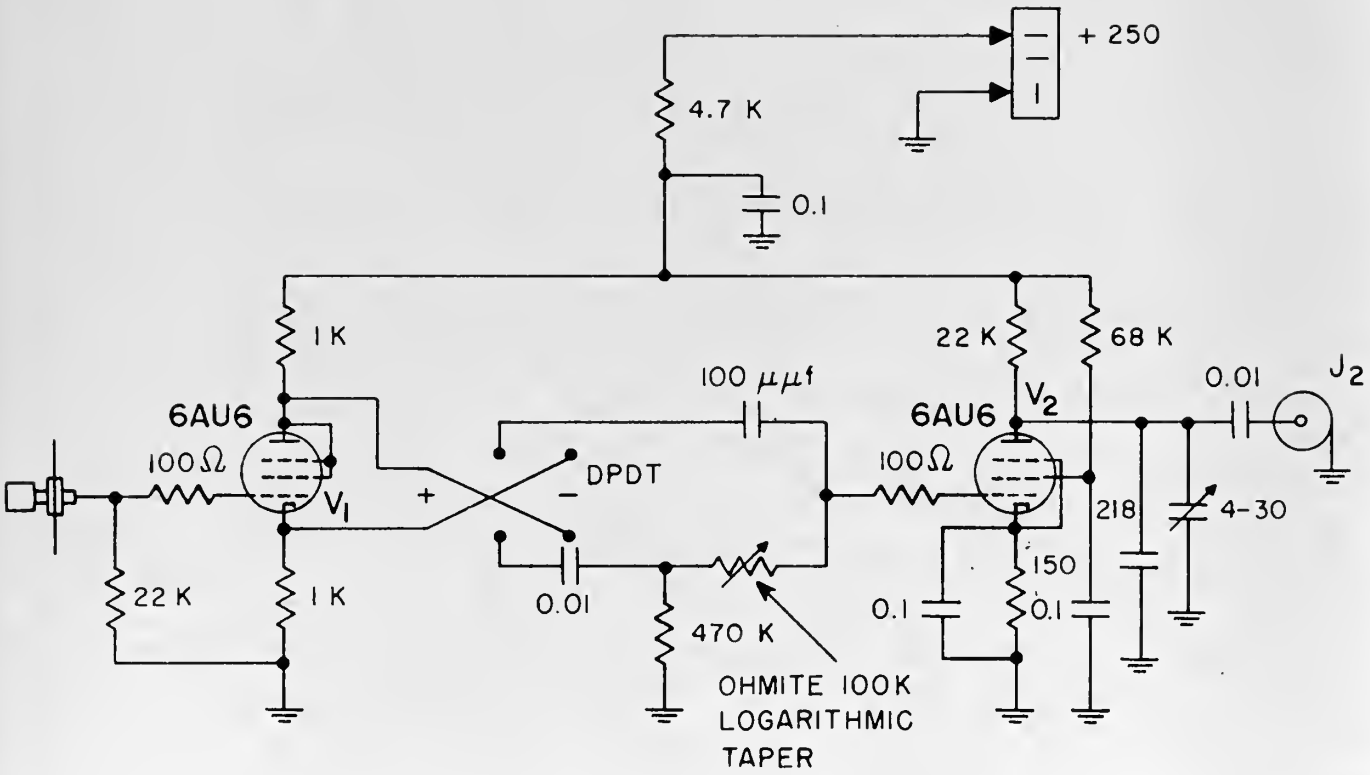

FIG. 25

PHASE SHIFTER CIRCUIT

A-591-TR40-432

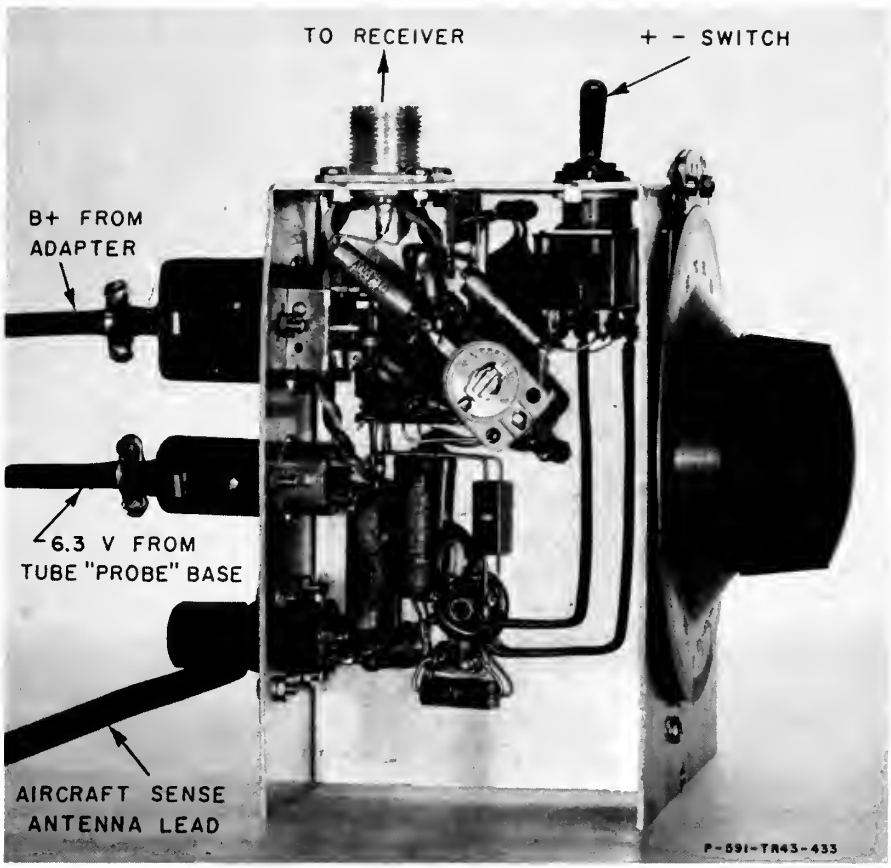

FIG. 26
PHASE SHIFTER

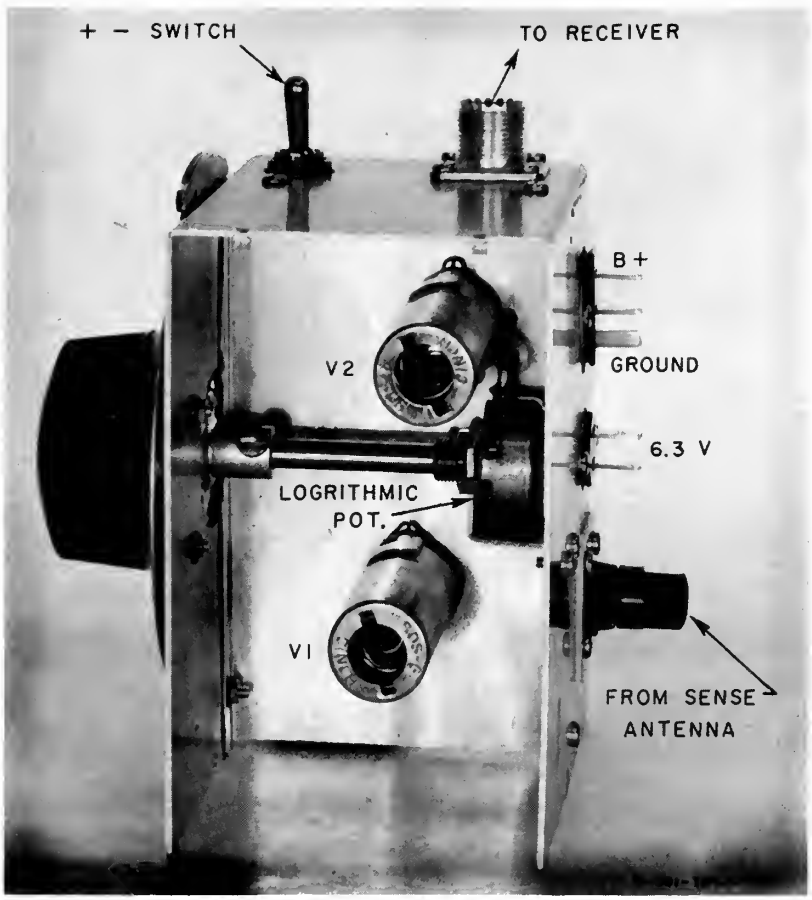

FIG. 27

PHASE SHIFTER

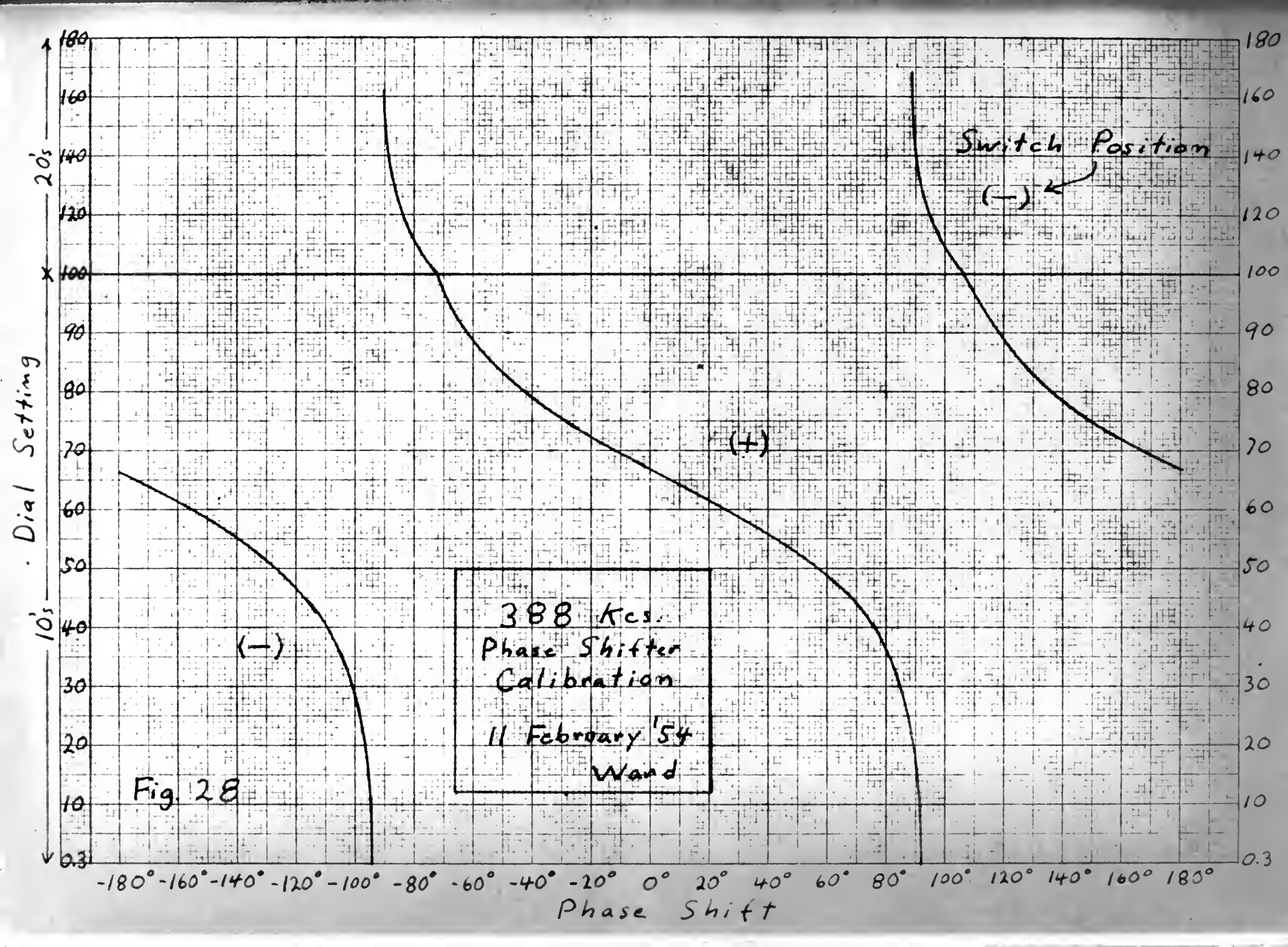
Switch Position
(−)
(+)
(−)
388 Kcs.
Phase Shifter
Calibration
11 February '54
Ward
Fig. 28
Dial Setting
10's
20's
180
160
140
120
100
90
80
70
60
50
40
30
20
10
0.3
-180° -160° -140° -120° -100° -80° -60° -40° -20° 0° 20° 40° 60° 80° 100° 120° 140° 160° 180°
Phase Shift

The variation of gain at a given frequency is caused by the variation of the phase shifter dial potentiometer.

The phase shift angle was found to be quite insensitive to the B+ voltage supplied. The supply voltage was varied from 40v to 250v with no noticeable effect on the phase shift.

The capacitors across the output of the phase shifter, driven by the pentode, V2, are necessary because the A.D.F. receiver is designed to be fed by an antenna-cable combination with a given capacitive value. In the case of the equipments used in these tests, this value is 270 uuf. The cable and cable connectors account for the rest of the 270 uuf.

When the circuit shown in Fig. 24 was constructed, before test "A", it was enclosed in the box shown in Fig. 29 together with the cable of "through wires," plug 122, the input binding posts, socket for the relay box cable, switches to cut the loop motor driving signal off to stop the loop in the position desired, additional switches to cut off the filter, and to cut off the signal to the recorder, plus potentiometers to set the level of the signal to the recorder. To get power for the phase shifter, the through wire carrying +250 d.c. was now tapped and the power brought to the shifter as shown in the various figures. Wires were soldered to the heater pins of one of the "tube probes" and the tubes of the phase shifter heated by this source. The through wire carrying +28 volts d.c. was tapped to give 28 volts to operate the chronograph pen of the recorder. The chronograph pen makes a mark on the margin of the recorder paper. It was used to mark the "over station" point and was operated by the switch shown in Fig. 31. The circuitry for the Adapter is shown in Fig. 30.

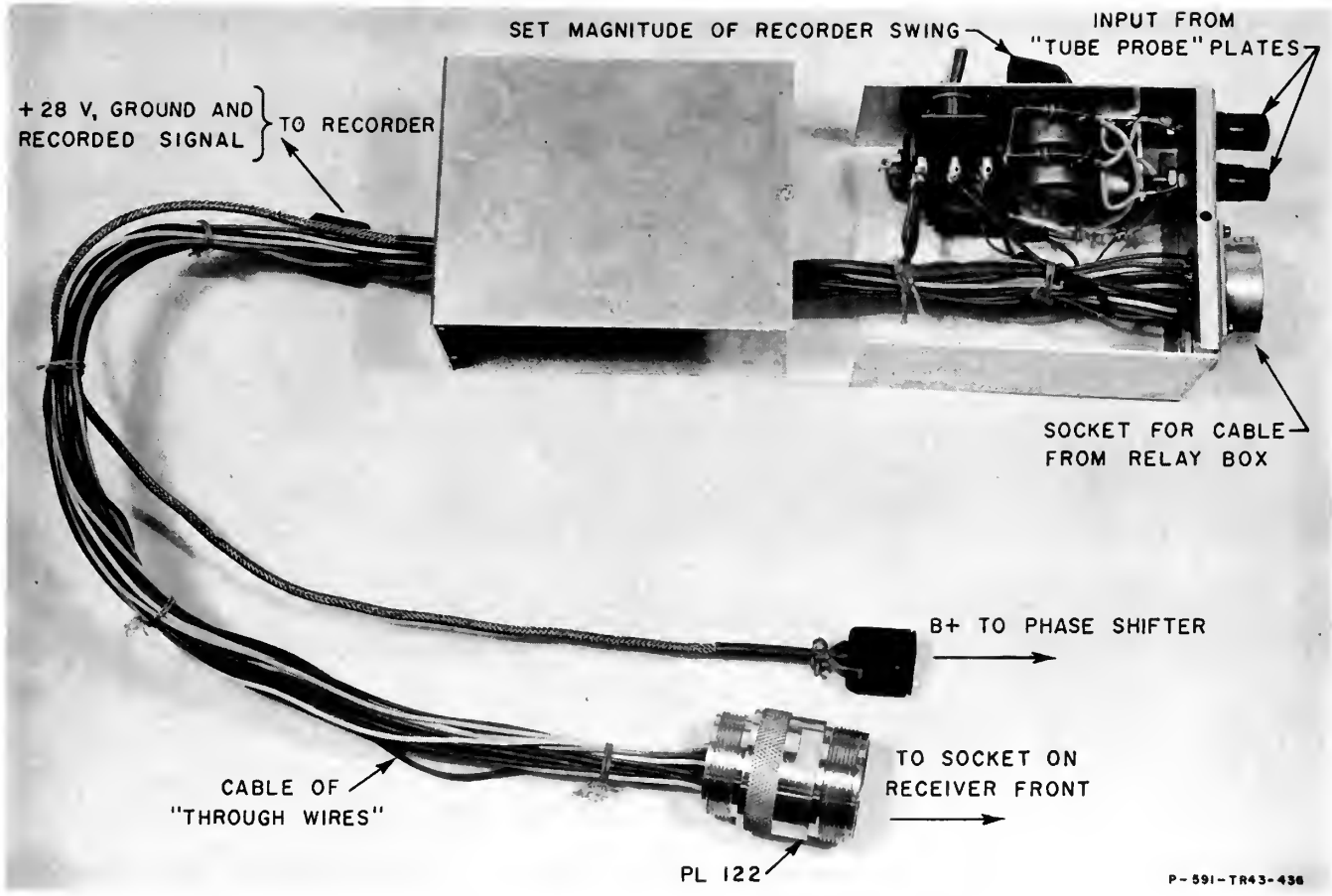

FIG. 29

ADAPTER

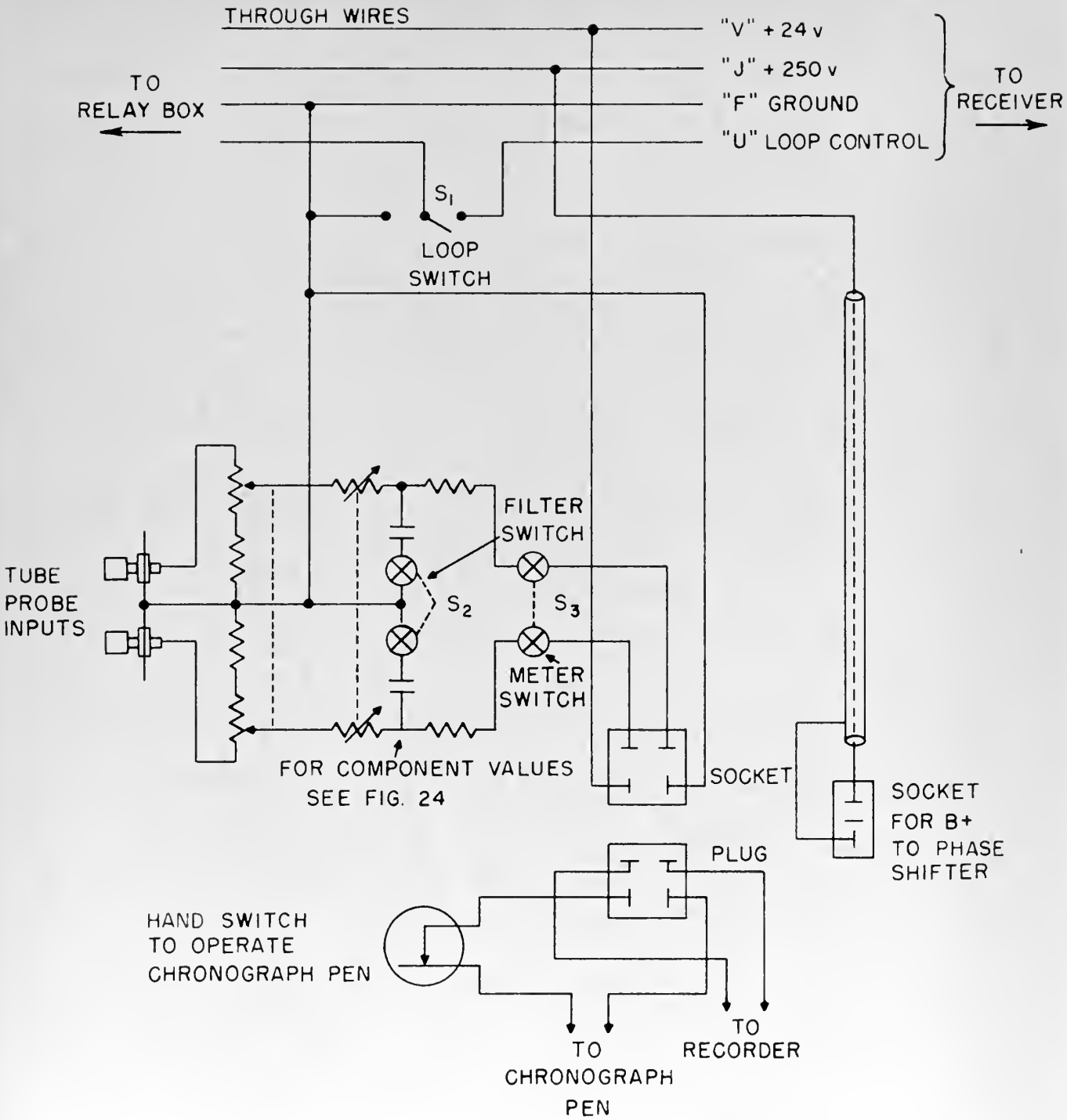

FIG. 30

ADAPTER CIRCUITS

A-591-TR40-437

When the phase shifter was completed and calibrated it was hooked up to the NA-1 receiver in the screened room. The receiver was then tuned to a signal generator signal at 357 Kc. The phase shift of the receiver was measured in the following way. The phase shifter was varied until the loop could be turned by hand to any bearing, and would stay stationary. In this condition the loop signal as shifted by the receiver and the sense signal as shifted by our phase shifter are 90° apart. Let us call the shift angle of this setting σ . The plus-minus switch was set to give $|\sigma| < 90^{\circ}$. In this condition the phase shift, γ , could be read as shown in Fig. 32. It was found to be 91°. With the receiver tuned as high as possible without losing the signal, γ , measured 120°; tuned as low as possible it measured 80°. This confirmed the conjecture made after Test "B".

The over all test equipment set up, used in the subsequent tests, is shown in Fig 31. All the connections to the receiver are shown to the left of the figure. The equipment can be connected and the ADF put back into normal operation within 10 minutes, provided the ADF is equipped with the 22 pin Cannon connector shown. All the military ARN-7's and allied types checked were so equipped. The NA-1 uses a different type, a 23 pin connector.

The recorder used for these tests was an Esterline Angus Model A.W. with a 3 milliampere movement. This Model is spring powered.

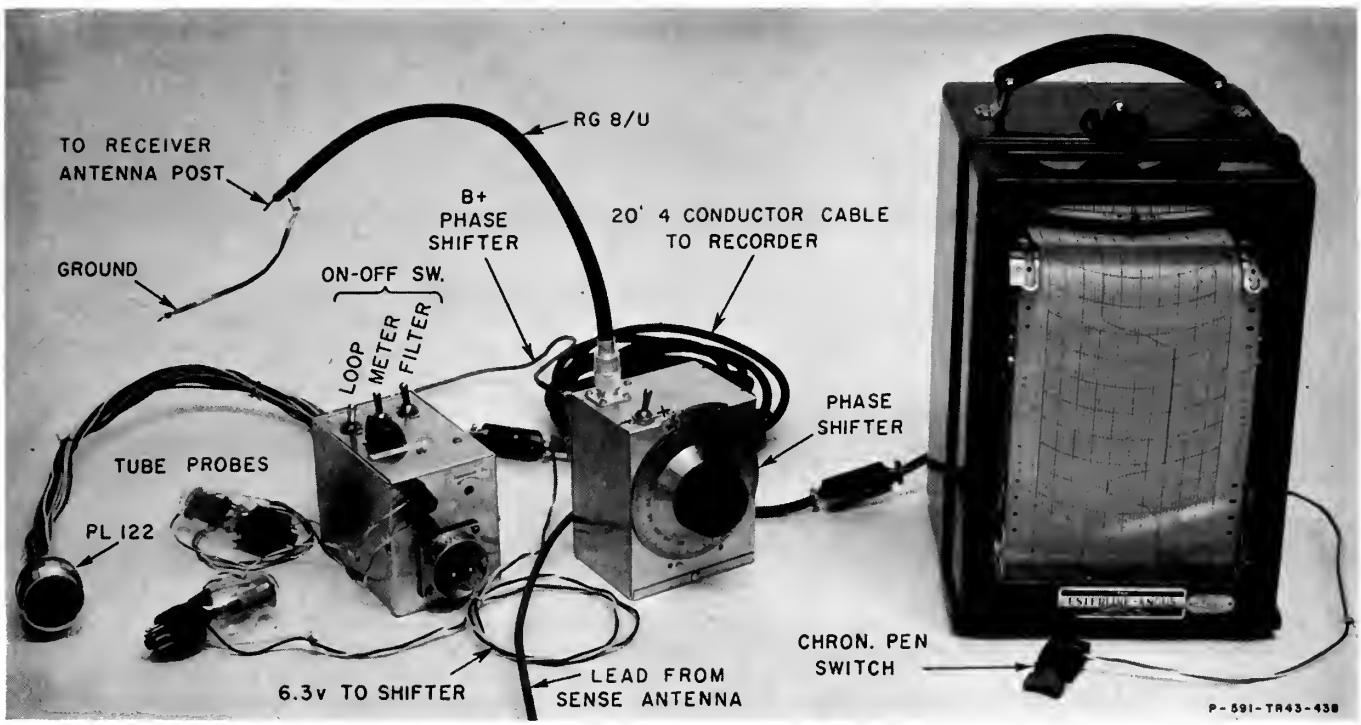

FIG. 3a

TEST EQUIPMENT CONNECTIONS

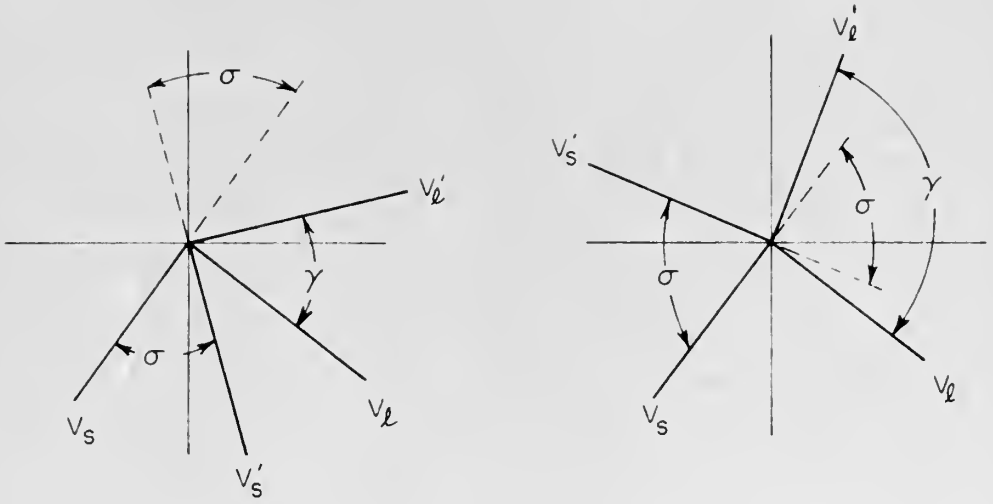

CASE 1 $\gamma < 90°$

(σ IS POSITIVE)

$\gamma = 90° - (90° - \sigma)$

$\gamma = \sigma$

NOTE:
$|\sigma| < 90°$

CASE 2 $\gamma > 90°$

(σ IS NEGATIVE)

$\gamma = 90° + (90° - |\sigma|)$

$\gamma = 180° - |\sigma|$

FIG 32

DEMONSTRATION OF THE METHOD OF MEASURING γ BY FINDING σ, THE PHASE SHIFTER ANGLE, WHICH SHIFTS V_S INTO PHASE QUADRATURE WITH V_{ℓ}'

A-591-TR40-439

2. Test Procedure

After the test equipment had been connected to the receiver and the aircraft had reached the vicinity of the station, the plane was flown to a point some 7 to 10 miles from the station at about 5000 ft. The station was tuned in for maximum signal with the phase shifter set for zero phase shift. This setting of the ADF dial was never touched for the remainder of the flight. The phase shift, γ, was then measured with the phase shifter using a procedure similar to that given in the latter part of the previous section. The aircraft was headed for the station, the loop trained abeam to the left, and the loop switch on the adapter tuned off. The function switch in the ADF central box must be on "Compass" for the tuning operation above and throughout the tests.

The turning signal put out by the thyratrons will now be at its maximum. This maximum is determined by the action of the AGC. The recorder was set mid-scale, 0.5, and the "meter" switch on the adapter turned on. The swing of the needle was set to 0.7 or 0.3, with the "inc. - dec." knob on the adapter, depending on the polarity of the input to the recorder. The desired γ was set. For example if the measured phase shift of the receiver was 95° and the desired γ for the run was 120°, then the phase shifter was set to shift the sense signal -25°. This would have the same effect as advancing the loop signal 25°. Likewise when a γ of 80° was desired, the sense antenna signal was advanced 15°.

On the ground at the station sight an assistant with a portable radio gave the aircraft a "mark" when it was, as closely as he could determine, over the station. This "mark" was transferred to the recording paper by the chronograph pen. The paper speed was four seconds between each heavy line. The paper was stopped between runs.

On each run the following were recorded: indicated airspeed, indicated altitude, outside air temperature, magnetic heading, and the γ used. On the ground the assistant made a note of any lateral deviation. He determined the instant of station passage by sighting up a vertical object.

Let us now examine the variables of Eq. 16(a) and note how each is established for the experimental checks.

h - computed from corrected altitude of aircraft, elevation of station sight, and the radio frequency of the station.

p - $\sqrt{x^2 + b^2}$

x - computed from corrected ground speed, the time on recorder trace from station passage, and the radio frequency.

b - controlled by pilots flying over known landmarks.

γ - set as desired

α - fixed by aircraft. Variable if another antenna were used. It's value was determined later by the weight of evidence of the experimental data.

CHAPTER V

EXPERIMENTAL RESULTS

From the recorder tracings made for each run and from the other data recorded, the points of sense transition were computed.

Sample recorder tracings are shown in Figs. 33 and 34. On the ARN-7 runs there is some inaccuracy due to the jitter of the trace mentioned in the previous chapter. Test "D" did not suffer from this trouble. Inspection of the sample traces shows that the apparent zero of the system is not at 0.5 (mid scale on the recorder) but about 0.55. The following laboratory calibration was made to determine the system zero. The recorder and adapter were connected and the same source of voltage fed to both "probe tube" input binding posts on the adapter. The controls of the adapter were set in the same position as when the flight test runs were made. When the voltage source was set to the approximate value of the zero signal d.c. level of the plates of the thyratrons, the recorder pen was at about 0.55. As the points of sense transition are located at the points where the recorder trace passes the "zero" line, this slightly indefinite zero would lead to some inaccuracy. The actual zero used in reading the recordings of all of the tests was the mean position between the A.V.C. limited portions of each trace, viz., in the case of Fig. 33(a) the zero is at 1/2 (0.3 + 0.8) or 0.55. In most cases the trace crosses the zero line at a fairly sharp angle however, and this reading inaccuracy does not lead to a very large position inaccuracy. Other data inaccuracies were the difficulty of passing directly over the station, the error in the ground observer's determination of the exact instant of passage at very low or very high altitudes, and the error in the wind data used.

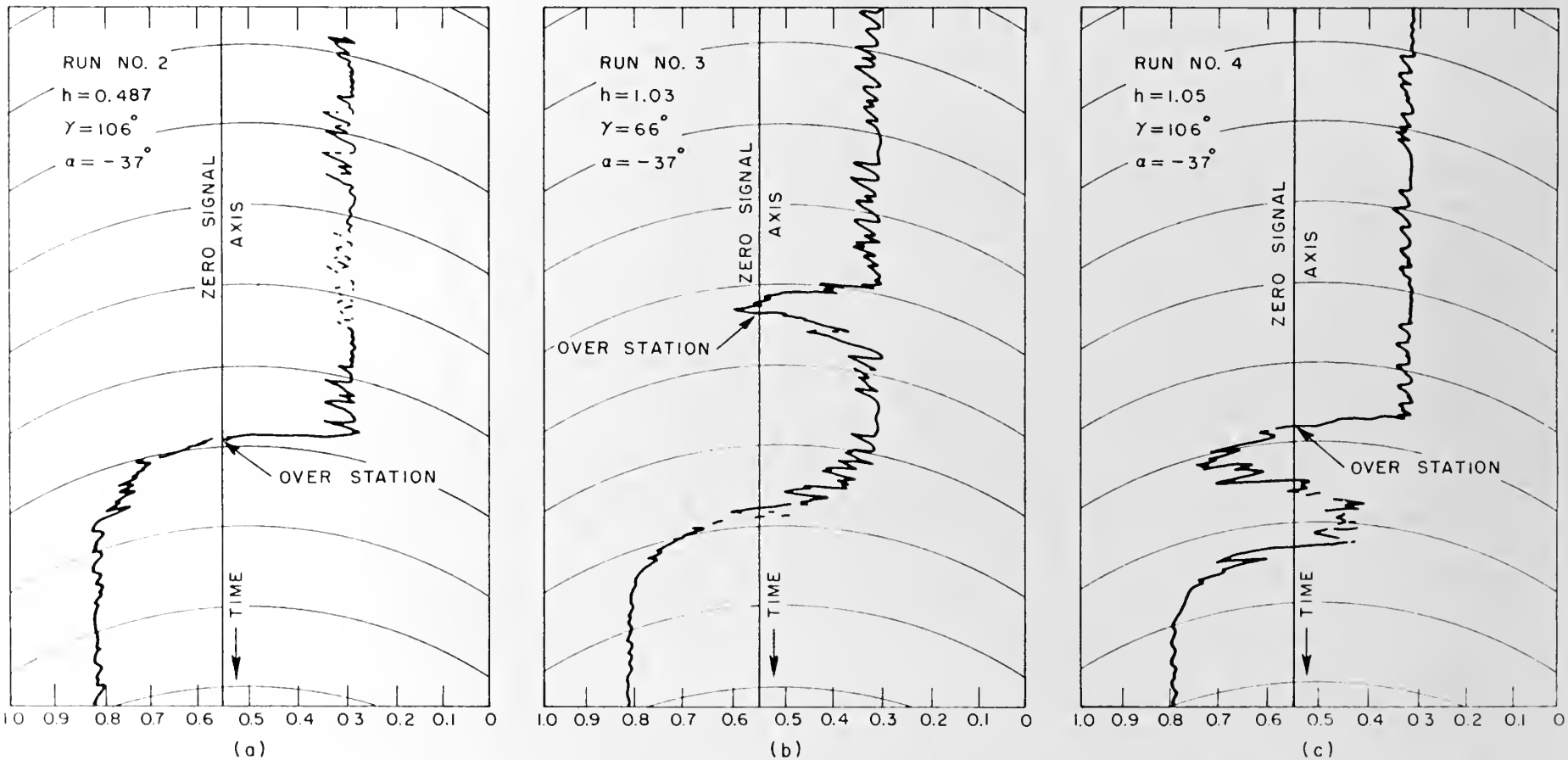

FIG. 33
SAMPLE RECORDER TRACINGS
TEST "C"

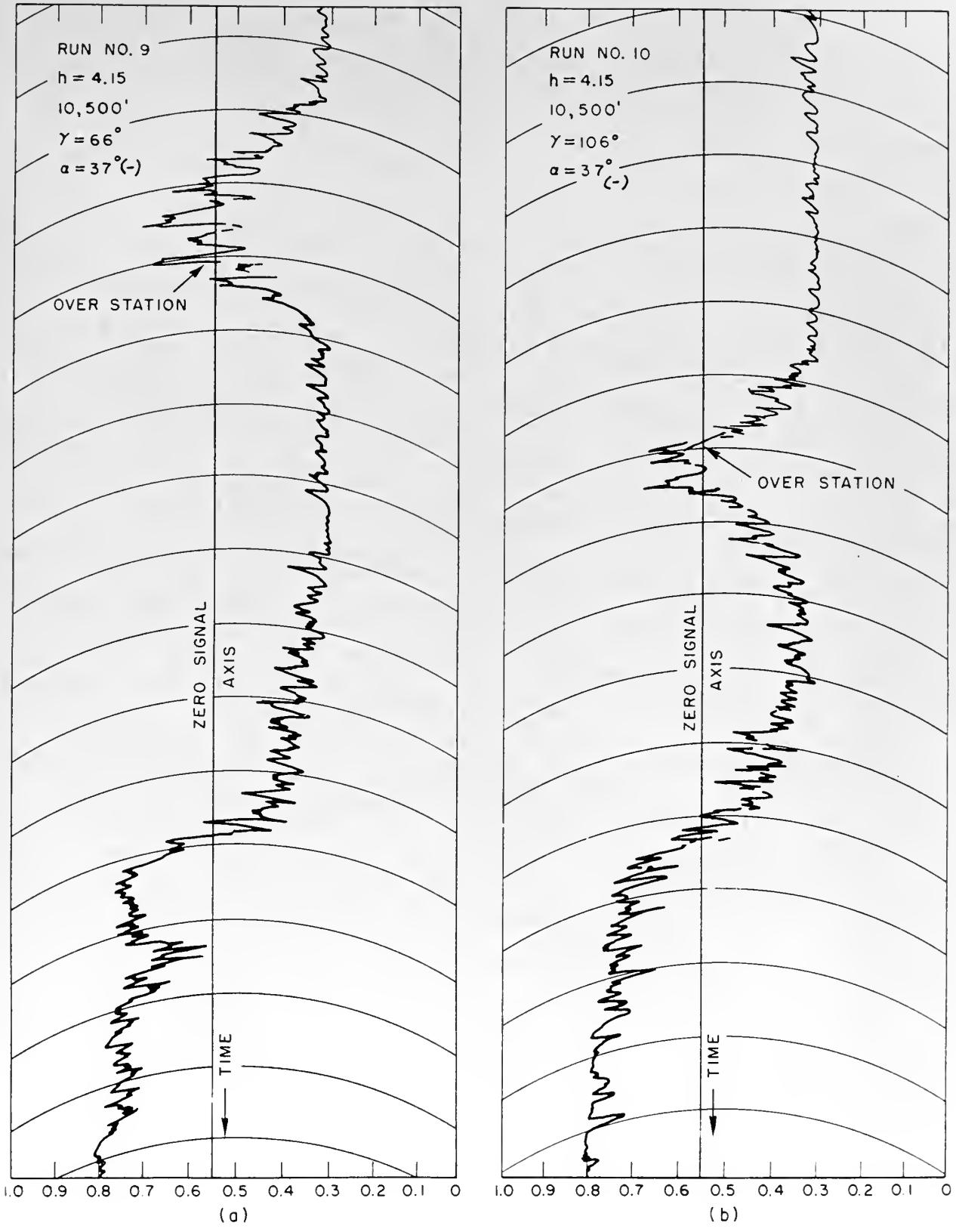

FIG. 34

SAMPLE RECORDER TRACINGS
TEST "C"

C-59-TR4 44

The results of Tests "C" are shown in Fig. 35 plotted together with the theoretical curves. Notice particularly the two points at h = 1.05 on the $\gamma = 106^{\circ}$ curve and the absence of any transition (dotted line) at h = 0.48 when γ was 106°. At h = 4.15 there are two points which seem to fall too far inside of the theoretical curve. The ground observer reported that the aircraft was considerably off to the left on this run. These two points are plotted in Fig. 36 with the horizontal cross section of the theoretical space figure for $\gamma = 106^{\circ}$, h = 4.15. We can see that the points fall near the circle. The angle by which the station zenith was missed, θ min, was 13.5° in this case. The altitude was 10,500 feet.

Test "D" was run over the radio range station at Oakland which is an Adcock range. The experimental data shows that, except right on the station axis, the ADF responds to the Adcock the same as it does to the single short radiator. There were two places, at h = 1 on the $\gamma = 70^{\circ}$ curve and at h = 4 on the $\gamma = 110^{\circ}$ curve of Fig. 37., where the recorder trace came to a minimum but did not cross the zero line over the station. Except for these points, the center radiator of the Adcock seemed to be the controlling factor. This effect of the Adcock is easily explained. The resultant horizontal magnetic field of the side towers and the resultant electric field of the side towers, which are in control when the aircraft is exactly over the center tower, do not exhibit a rapid change of direction or a reversal of phase as the center tower axis is passed. Therefore there would be no sense transition. In other words, the center tower is in control of the ADF except during that small period when the magnetic field of the center tower is so small that the resultant magnetic field of the side towers produces a much stronger signal in the loop. For this short time the ADF is controlled by the resultant magnetic

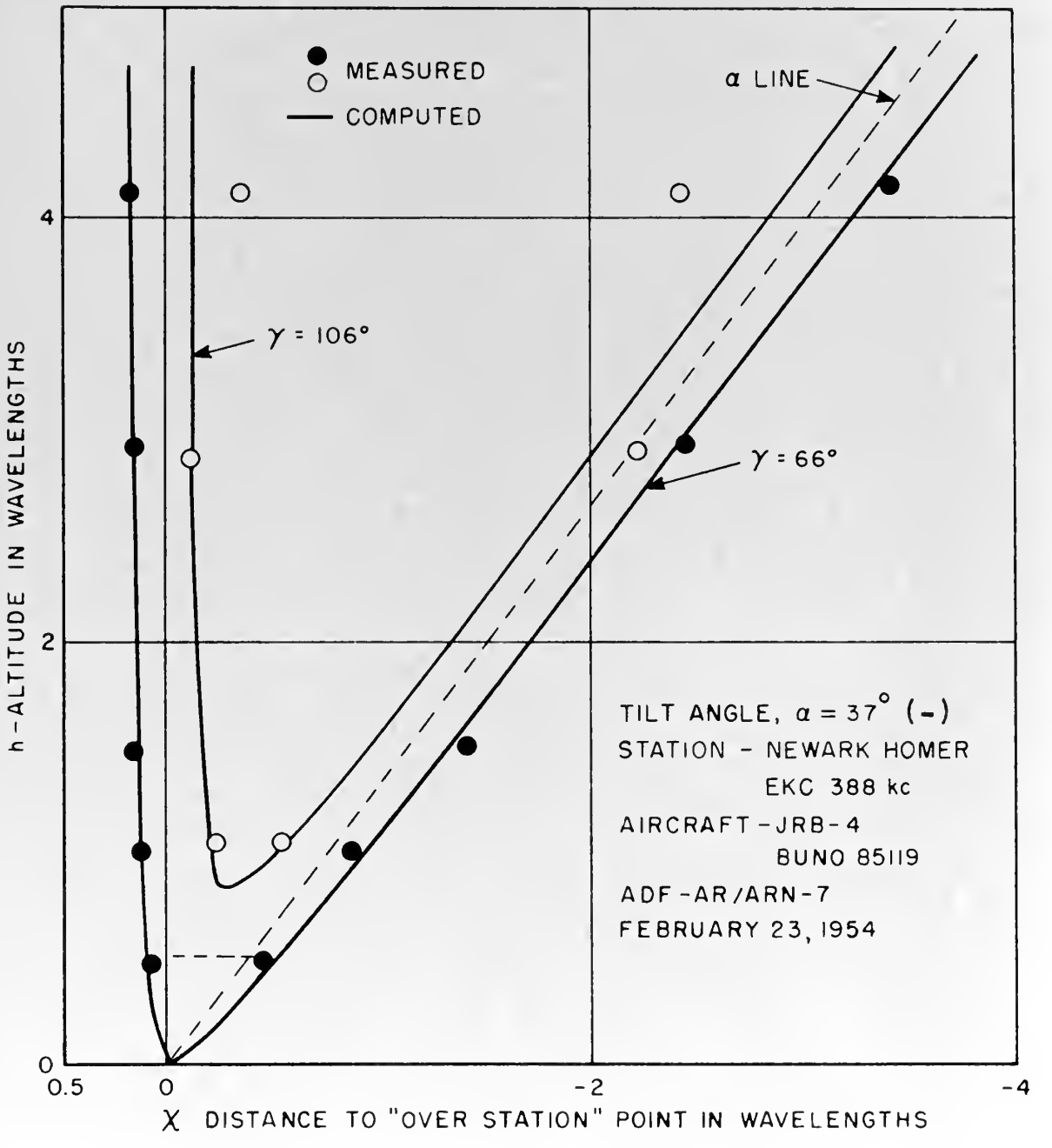

FIG. 35

EXPERIMENTAL RESULTS PLOTTED ON THEORETICAL CURVES FOR A SINGLE VERY SHORT VERTICAL TOWER AS GROUND RADIATOR. TEST "C"

A-591-TR40-442

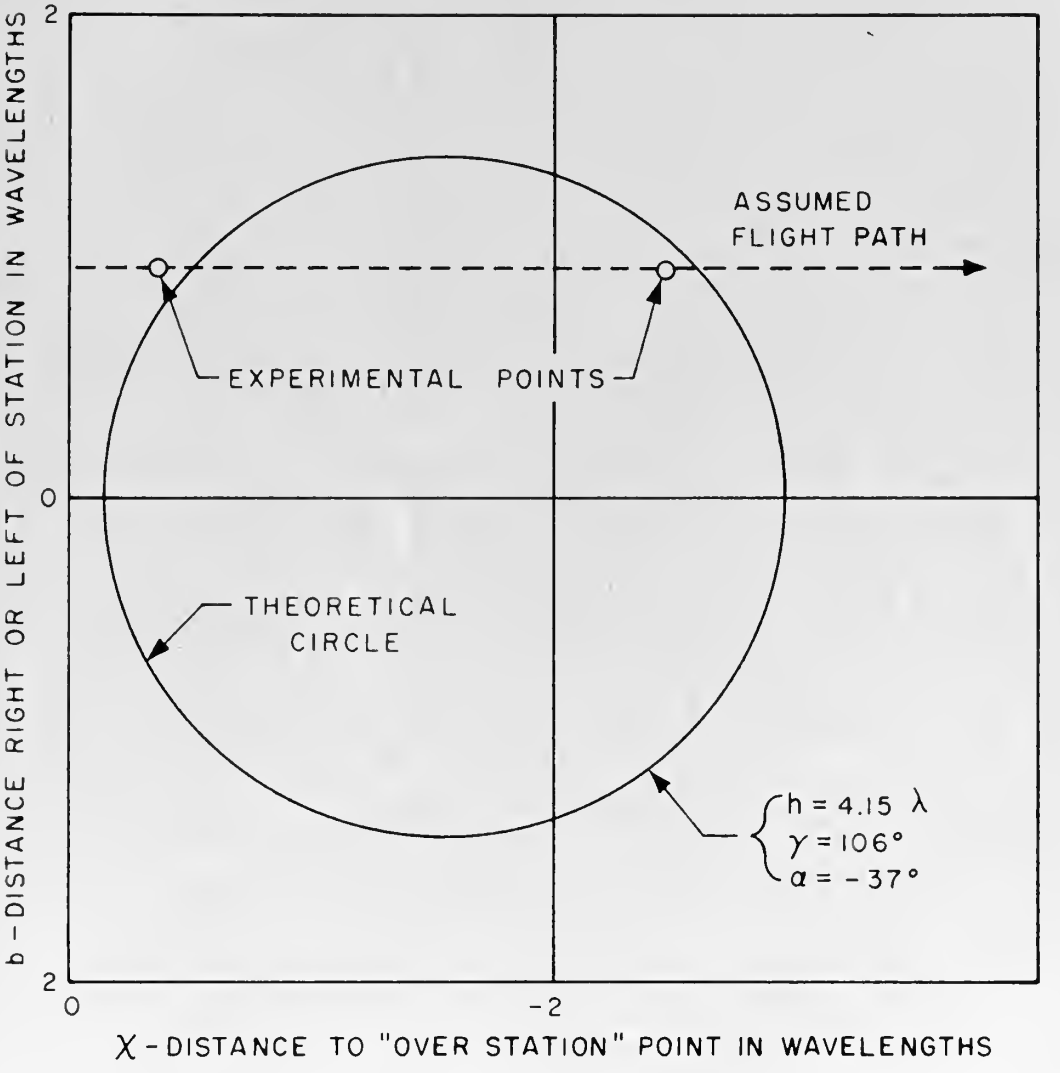

FIG. 36

POINTS AT $h = 4.15\lambda$ FROM FIG. 35 PLOTTED ON THEORETICAL CIRCLE. ACTUAL ALTITUDE 10,500 FEET.

A-591-TR40-443

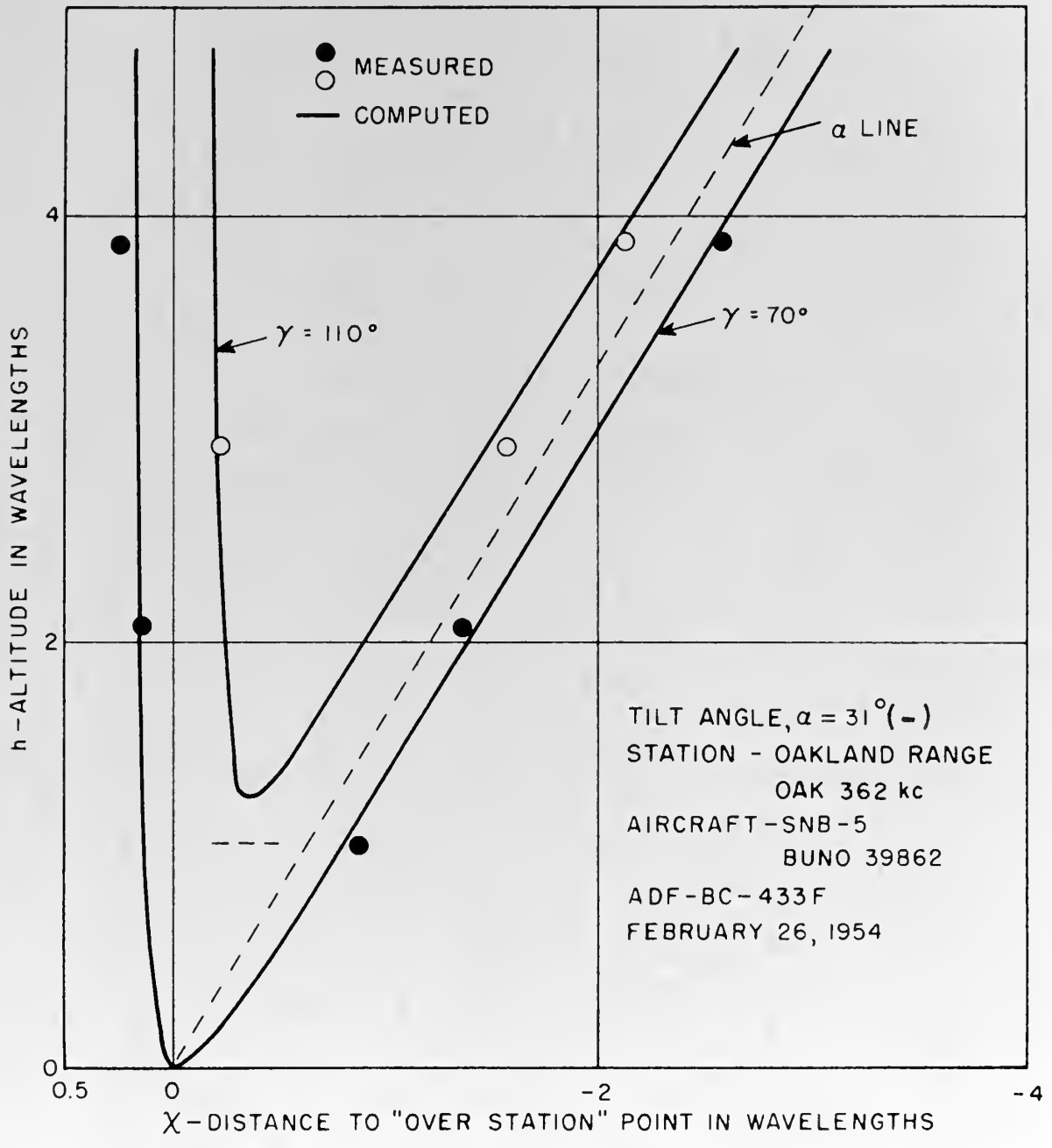

FIG. 37

EXPERIMENTAL POINTS PLOTTED ON THEORETICAL CURVES FOR AN ADCOCK RANGE STATION AS GROUND RADIATOR. TEST "D"

A-591-TR40-444

field of the side towers and the resultant electric field of the side towers. There is no effect produced in the servo system by the combination of the loop voltage due to the magnetic field of the side towers and the sense antenna signal due to the electric field of the center tower for these two fields are varying at frequencies differing by 1020 cps, while the time constant at the servo system is of the order of seven seconds.

This effect is of no consequence for it will not give additional points of transition; it may slightly displace one or it may eliminate two, the loop transition and that sense transition nearly over the station. As shown in Fig. 37 the space figure tip behaves the same as was predicted on the basis of the theoretical data. The $\gamma = 110^{\circ}$ run at h = 1 produced no sense antenna transitions.

In Fig. 38 are shown the paths of two passes made wide of the station at h = 1.05 during Test "D". The horizontal section of the $\gamma = 70^{\circ}$ space figure is shown to confirm the two single transition traces obtained.

The experimental data show excellent agreement with that predicted by Eq. (16a) and it is felt that this agreement more than adequately supports the theoretical findings of this investigation.

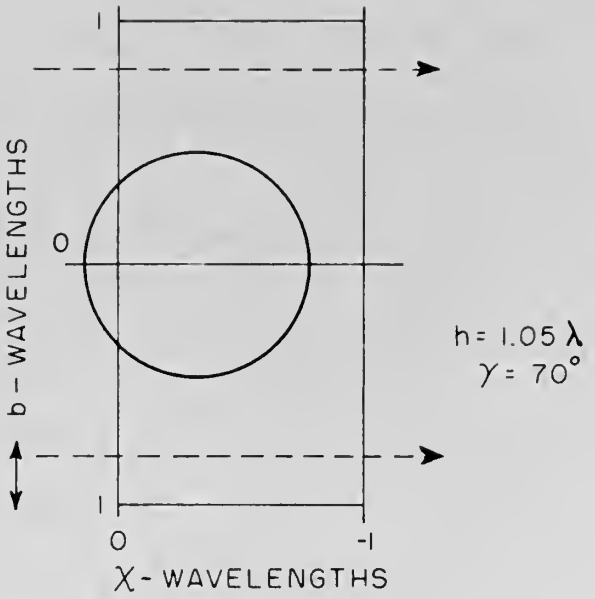

FIG. 38

TRACKS OF TWO RUNS MADE 0.82 EACH SIDE OF THE STATION DURING TEST "D", h= 1.05, PLOTTED RELATIVE TO THE CROSS SECTION OF THE THEORETICAL SPACE FIGURE

A-591-TR40-445

CHAPTER VI

CONCLUSIONS

In the preceding chapters we have investigated the reasons, based on field theory and the electrical characteristics of the equipment and the aircraft, for the multiple reversals of the airborne radio compass indicator as the aircraft passes near or over a ground radio station to which it is tuned. These multiple reversals give position inaccuracies which, even in practical systems, may be equal to or more than the altitude of the aircraft, and in any case do not give a sure indication of the instant the ground station axis is passed. At high altitudes, although it would be convenient to know the exact time of station passage, it is not as important as knowing this fact at low altitudes such as on airport approaches for example. These investigations have indicated a possible solution to this problem.

A study of Figs. 14 through 21 shows that at some altitude, depending on the wavelength of the station under consideration, the tilt angle of the effective aircraft sense antenna, and the overall receiver phase advance of the loop signal relative to the sense antenna signal, we may find a point below which the sense antenna signal will never be in time quadrature with the shifted loop signal. This being true, there will not be any compass reversals due to the sense antenna signal phase shift because the point of phase quadrature is the sense antenna phase transition point. The only compass reversal will be that due to the loop transition when the aircraft passes over the station. The above phenomena will only occur if the phase shift angle, γ, is greater than 90°. Fig. 22 gives the plotted relationship between the altitude in wavelengths, h,

the tilt angle, α , and the phase shift, γ . From this figure we can pick the phase shift required to give us a single compass reversal at or below a given altitude at one frequency. From a practical point of view we require a system that would give us a single reversal over the station at or below a given altitude at any frequency in the useable ADF band. To accomplish this we would need a phase shifter to replace the calibrated phase shifter used in the flight tests reported in the previous chapters. This phase shifter would have to be designed to give a phase shift that varied with frequency in such a way that the altitude of our space figure tip was constant or nearly so.

Substituting $h = z/\lambda$ in Eq. (19a) and rearranging we have:

$$z = \frac{\cos\frac{\alpha}{2}}{\pi \tan^2\frac{\alpha}{2}} \cdot \frac{\lambda}{(-\tan\gamma)} \qquad (19b)$$

as the formula for the altitude of the space figure tip. The tilt angle, α , is a constant in any installation. For z to be constant, $\frac{\lambda}{-\tan\gamma}$ must be a constant.

$$-\tan\gamma = \frac{\lambda}{k}$$

The phase shifter in the receiver gives a phase shift of nearly 90° when the receiver is carefully tuned. The phase angle, γ , would be $90^\circ + \gamma'$ where γ' is the amount by which the required γ is greater than 90°.

$$-\tan(90^\circ + \gamma') = \frac{\lambda}{k}$$

$$\cot\gamma' = \frac{\lambda}{k}$$

$$\tan\gamma' = \frac{k}{\lambda} = \frac{k}{c} f$$

In short, to keep the tip of the space figure at a constant altitude regardless of frequency we would need a shifter which would produce a negative phase shift (to be applied to the sense antenna signal) and in which the tangent of this phase shift angle was proportional to the frequency of the radio frequency signal. The gain of this shifter should be small but greater than unity.

There is another approach to the phase shifter problem, an empirical one. Again checking Fig. 22 we see that, for a tilt angle of 20°, a γ of 120° will give us a space figure with its tip at h = 6 . At a frequency of 1750 kc this is about 3400 feet. The basic shifter circuit included in Fig. 25, with the "plus-minus" switch on plus, has the property that its shift angle is given by:

$$(-)\ 2 \tan^{-1} (\omega CR)$$

γ' would be 30° so that $\tan^{-1} \omega CR$ would be 15°.

$$\omega CR = 0.268 \text{ at } 1750 \text{ kc.}$$

At 200 kc ωCR would be 0.0306 and $\tan^{-1} \omega CR = 1.75^\circ$.

γ' would be approximately 3.5°; this would give a space figure tip at $h \approx 0.62$ or, at this frequency, some 3100 feet compared with 3400 feet at 1750 kc.

The phase shift of the actual shifter of Fig. 25 varied at about three times the required rate with respect to frequency due to other phase shifting elements in the circuit. It is felt that this is an engineering problem and that perhaps a very simple phase shifter could be developed, getting its heater and plate voltage supply from the parent receiver, which could be put in a box chassis of dimensions about 1.5" x 1.5" x 1.5". This unit could have a binding post on it for the sense antenna lead and be supported on the front of the receiver unit by a 4 pin AN type plug

which could be rigidly mounted on this small unit. The socket for this plug could replace the present antenna post of the ADF receiver.

The shifters discussed above are designed to go on the present ADF systems with little modification. A new ADF system could incorporate the shifter as an integral part of the receiver.

An interim and very simple solution to the phase shifter problem is suggested by the phase shift effect of receiver tuning suspected during test "B" and verified after the calibrated phase shifter had been built. By tuning in any station so that the dial reading is higher than the reading of the point of maximum signal, say to such a high reading that the tuning indicator drops back to 0.7 of the maximum signal position, the total phase shift will be more than 90°. Using this tuning procedure, approximately fifty runs have subsequently been made over stations covering the entire ADF band. The runs were made at or below one and a half wavelengths of altitude. In all of these cases a single transition, over the station, was obtained. This technique has the advantage of material simplicity but the disadvantage of being a tuning technique and subject to operator error.

Another consideration is the effect that a permanent phase shift greater than 90° would have on the extreme range performance of the ADF. At long ranges the torque which turns the loop varies as the sin γ . Even the 30° additional shift proposed at 1750 kc would reduce the torque to 0.866 of its $\gamma = 90^{\circ}$ value. This would be a significant reduction.

The above paragraph adds weight to the following proposal. There is a conflict between the "close-in" characteristics and the long range characteristics of the ADF. Close-in work needs a small tilt angle, a shorter time constant for the loop drive motor so that it may respond more rapidly in the strong signal areas, and a phase shift of more than 90°.

The long range work needs a short sense antenna lead to reduce losses as discussed previously, a longer time constant to damp out the wandering of the compass due to interference at long ranges, and a phase shift of 90°. A single switcher could be developed which would be activated by signal strength, which could be tripped by push button if desired, which would have about a one-minute delay so that it would not switch to "long range" during momentary losses of signal, and which would shift to a forward sense antenna mounted near the receiver and shift to $\gamma = 90^{\circ}$ for weak signals. When the average signal strength reached a certain value the switcher would shift to a small sense antenna under the electrical center of the aircraft, shift to the $\gamma > 90^{\circ}$, and triple the drive speed of the loop.

It is felt that the above proposal based in part on the results of the investigations of this project would materially improve the operation of the ADF.

BIBLIOGRAPHY

1 - AEEC Letters 54-1-11 and 54-1-11A of November 1953, "Some Considerations Regarding the Use of a Unity-Gain Sense Antenna Coupling Amplifier For ADF Receivers", and Test Report on a Unity-Gain Sense Antenna Coupling Amplifier for ADF Receivers.

2 - Bolljahn, J. T. - "Low-Frequency Aircraft Antennas" in Report of the Feb. 7th (1953) meeting of Airlines Electronic Engineering Committee (AEEC) prepared by the Stanford Research Institute.

3 - Bolljahn, J. T., "The Measurement of Low-Frequency Aircraft Antennas Properties Using Electrostatic Techniques." Technical Report No. 19, Air Force Contract No. AF 19(122)78. September 1951.

4 - Bolljahn, J. T., "Antennas For Airborne ADF Systems," Interim Report on Task II, Air Force Contract No. AF 33(038)-7850. February 1952

5 - Granger, J. V. N. "Design Limitations on Aircraft Antenna Systems" from Aeronautical Engineering Review of May 1952.

6 - Hoblitzell, C. M. "Effect of Airframe Configuration on Low-Frequency Antenna Characteristics." Technical Report No. 38, Air Force Contract No. AF 19(604)266, April 1953.

7 - Schelkunoff, S.A., and Friis, H.T., "Antennas: Theory and Practice."

8 - Wright Air Development Center Weapons Component Division. Exhibit No. WCEN-1004 of 19 December 1951, as amended to 19 March 1953.

9 - Instruction Book for Type NA-1 Aircraft Navigation System - Bendix Radio.

10 - An 16-30ARN7-3 Handbook and Maintenance Instructions - Radio Compass AN/ARN-7

11 - NAVAER 16 - 40SCR269-504 Handbook and Maintenance Instructions - Radio Compass SCR-269-F

12 - AN 16-30ARN 6-3 Handbook and Maintenance Instructions - Radio Compass AN/ARN-6.

APPENDIX

In all of the preceding work with the field quantities we have disregarded the effect of the third term of E_θ as given in Eq.(1). The points where the radio compass starts to reverse are those where the phase of the voltage in the sense antenna is 90° to the voltage of the loop after the loop voltage has been advanced in phase by the receiver. The only significent effect that the third term of E_θ could have would be to alter the phase of the sense antenna voltage. The phase of the voltage in the sense antenna is a function of the location and orientation of the sense antenna in space. The effect of slightly changing this phase will be of consequence only in the areas where the sense antenna and loop voltages are very nearly in time quadrature.

The equation for the unit voltage in the sense antenna was derived in Fig.4 and is:

$$V_s = E_z \cos \alpha + (E_\rho \cos \phi) \sin \alpha \qquad (13)$$

where

$$E_\rho = E_r \sin \theta + E_\theta \cos \theta$$

$$E_z = E_r \cos \theta - E_\theta \sin \theta$$

For use in this appendix only, primed values will be used to designate quantities in which the effect of the third term of E_θ is <u>not</u> considered.

From Eq.(1) and Eq.(3), letting $\delta = \frac{\lambda}{2\pi r}$ we have:

$$E_\theta = \frac{j\eta I_s}{2\lambda r}\epsilon^{(\ )}\left[(1-\delta^2) - j\delta\right]\sin\theta \qquad (1\ b)$$

$$E'_\theta = \frac{j\eta I_s}{2\lambda r}\epsilon^{(\ )}\left[1 - j\delta\right]\sin\theta \qquad (1\ b')$$

$$E_r = \frac{\eta I_s}{2\lambda r}\epsilon^{(\ )}\left[1 - j\delta\right] 2\delta\cos\theta \qquad (3\ b)$$

Using Eqs.(13), (1 b) and (3 b) and choosing a course directly over the station, $\phi = 0$, we can obtain an expression for V_s. From this the phase angle of V_s is then:

$$\angle V_s = \tan^{-1}\left[\frac{D - \delta^2(3D+2)}{\delta(3D+2)}\right] \qquad (23)$$

where $D = \sin\theta(\cos\theta\tan\alpha - \sin\theta)$

Using Eqs.(13), (1 b′) and (3 b) similarly we obtain:

$$\angle V_s' = \tan^{-1}\left[\frac{D - \delta^2(2D+2)}{\delta(3D+2)}\right] \qquad (23')$$

The error in phase of V_s caused by not considering the third term of E_θ will be:

$$\Delta = \angle V_s - \angle V_s' \qquad (24)$$

using $\tan(A - B) = \dfrac{\tan A - \tan B}{1 + \tan A \tan B}$

$$\tan\Delta = \frac{\delta^3 D(3D+2)}{\delta^2(3D+2)^2 + D^2 - D\delta^2(5D+4) + \delta^4(2D+2)(3D+2)} \qquad (24a)$$

$$\cot\Delta = \frac{\delta(2D+2)}{D} + \frac{3D+2}{\delta D} - \frac{5D+4}{\delta(3D+2)} + \frac{D}{\delta^3(3D+2)} \qquad (25)$$

If the coordinates of points on the curves of Figs. 14 or 16 are put in this equation, we will find that the magnitude of Δ will be less than 1° until the direct distance to the station is less than 0.1 wavelengths. The phase error, Δ , is effectively a modification of the phase shift angle, γ . By consulting Figs. 14 and 16 we can see that even if Δ were one degree, it would not noticeably affect the position of our space figure.

Perhaps the greatest effect of Δ would be the effect it would have on the altitude of the space figure tip when $\gamma > 90^{\circ}$. From Fig.22 we can see that a change of 1° would alter "h" somewhat. If the tilt angle were 15° and the phase shift were 100° instead of 99°, the height of the space figure tip would be 3.2 λ instead of 3.0 λ .

Inasmuch as we would have to get very close to the station (very low over the station) before Δ would be 1°, and inasmuch as even 1° would produce very little effect, we can omit the third term of E_{θ} from our calculations without introducing any practical error.